Int J Earth Sci (Geol Rundsch) (2010) 99:1827–1847
DOI 10.1007/s00531-009-0490-9

ORIGINAL PAPER

A new perspective on the significance of the Ranotsara shear zone in Madagascar

Guido Schreurs · Jörg Giese · Alfons Berger · Edwin Gnos

Received: 23 February 2009 / Accepted: 10 October 2009 / Published online: 18 November 2009

Abstract The Ranotsara shear zone in Madagascar has been considered in previous studies to be a >350-km-long, intracrustal strike-slip shear zone of Precambrian/Cambrian age. Because of its oblique strike to the east and west coast of Madagascar, the Ranotsara shear zone has been correlated with shear zones in southern India and eastern Africa in Gondwana reconstructions. Our assessment using remote sensing data and field-based investigations, however, reveals that what previously has been interpreted as the Ranotsara shear zone is in fact a composite structure with a ductile deflection zone confined to its central segment and prominent NW–SE trending brittle faulting along most of its length. We therefore prefer the more neutral term "Ranotsara Zone". Lithologies, tectonic foliations, and axial trace trajectories of major folds can be followed from south to north across most of the Ranotsara Zone and show only a marked deflection along its central segment. The ductile deflection zone is interpreted as a result of E–W indentation of the Antananarivo Block into the less rigid, predominantly metasedimentary rocks of the Southwestern Madagascar Block during a late phase of the Neoproterozoic/Cambrian East African Orogeny (c. 550–520 Ma). The Ranotsara Zone shows significant NW–SE striking brittle faulting that reactivates part of the NW–SE striking ductile structures in the flexure zone, but also extends along strike toward the NW and toward the SE. Brittle reactivation of ductile structures along the central segment of the Ranotsara Zone, confirmed by apatite-fission track results, may have led to the formation of a shallow Neogene basin underlying the Ranotsara plain. The present-day drainage pattern suggests on-going normal fault activity along the central segment. The Ranotsara Zone is not a megascale intracrustal strike-slip shear zone that crosscuts the entire basement of southern Madagascar. It can therefore not be used as a piercing point in Gondwana reconstructions.

Keywords Ranotsara shear zone · Madagascar · Tectonics · East African Orogen · Gondwana · Apatite fission-track dating

G. Schreurs (✉) · J. Giese
Institute of Geological Sciences, University of Bern,
Baltzerstrasse 1-3, 3012 Bern, Switzerland
e-mail: schreurs@geo.unibe.ch

A. Berger
Institut for Geografi og Geologi, Øster Voldgade 10,
1350 Copenhagen, Denmark

E. Gnos
Museum d'Histoire Naturelle, 1 Route de Malagnou,
1211 Geneve 6, Switzerland

Present Address:
J. Giese
Institut für Geologie und Paläontologie,
Westfälische Wilhelms-Universität Münster,
Corrensstr. 24, 48149 Munster, Germany

Introduction

The eastern two-thirds of the island of Madagascar consist predominantly of Precambrian to early Cambrian rocks. Most of these rocks have been reworked at high-grade metamorphic conditions during the East African Orogen (EAO of Stern 1994) that formed during assembly of the supercontinent Gondwana in late Neoproterozoic/early Paleozoic times (Stern 1994). The Precambrian to early Cambrian rocks are the crystalline basement to late Carboniferous to Neogene sedimentary and volcanic sequences that were deposited during and after rifting and drifting of

Gondwana since late Paleozoic times. It is widely accepted that Madagascar occupied a central position within the former supercontinent Gondwana (Fig. 1), sandwiched between India and eastern Africa (e.g. Stern 1994; Lawver et al. 1999; Veevers 2001; Reeves et al. 2002, 2004; Collins and Windley 2002; MacDonald et al. 2003; Collins and Pisarevsky 2005; Collins 2006).

Constraints on a more precise paleoposition of Madagascar in the early Paleozoic are often inferred by correlating structural features in particular steeply dipping shear zones that formed prior to Gondwana break-up. In Madagascar, major zones with (sub)vertical foliation planes (Fig. 2) have been interpreted as ductile shear zones (e.g. Windley et al. 1994; Martelat 1998; Martelat et al. 2000; Nédélec et al. 2000) that formed at high-grade metamorphic conditions during the late stages of the East African Orogen (Nicollet 1990; Martelat et al. 1997; de Wit et al. 2001). Although the steep ductile zones predominantly strike N–S (present-day coordinates), previous workers also postulated a NW–SE striking ductile shear zone that traverses the entire crystalline basement of southern Madagascar (e.g., Katz and Premoli 1979; Ackermand et al. 1989; Martelat 1998). This zone is generally referred to as the Ranotsara shear zone, but has previously also been termed Ranotsara–Ranomena lineament (Katz and Premoli 1979), Ranotsara shear belt (Ackermand et al. 1989) or Bongolava-Ranotsara shear zone (Caen-Vachette 1979; Martelat 1998; Lardeaux et al. 1997, 1999; Müller 2000). It is generally regarded as a ~20-km-wide intra-crustal strike-slip shear zone (Martelat et al. 2000) with a sinistral sense of shear (e.g. Nicollet 1990; Windley et al. 1994; Martelat et al. 1997; Martelat et al. 2000; de Wit et al. 2001) and an exposed length of about 350 km (Martelat et al. 2000). Because of its oblique orientation with respect

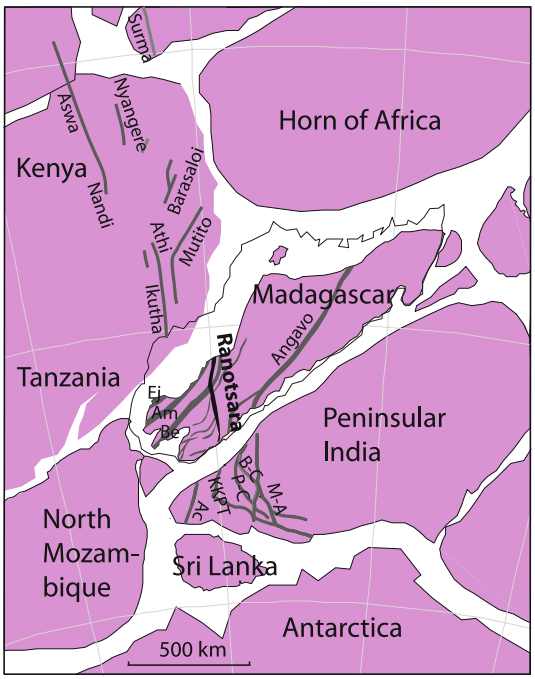

Fig. 1 Madagascar and its position within a central Gondwana reconstruction 250 Ma (modified from Reeves 2008, unpubl., model CR09MZRJ.rot, which is an updated version of model reev519c published in Reeves et al. 2004). *Purple* geometrically rigid Precambrian continental crust, *white* areas of continental crust that have been extended and lost from outcrop by rifting, *dark grey* zones with steep foliations that have been interpreted as ductile shear zones. Data from Madagascar compiled after Martelat (1998), Martelat et al. (2000), Nédélec et al. (2000), and de Wit et al. (2001); data from southern India after Ghosh et al. (2004) and data from eastern Africa after Bonavia and Chorowicz (1993), Mosley (1993) and Smith and Mosley (1993), *black* location of the Ranotsara Zone. *Ac* Achankovil shear zone, *Am* Ampanihy shear zone, *B–C* Bhavani–Cauvery shear zone, *Be* Bereketa shear zone, *EJ* Ejeda shear zone, *KKPT* Karur–Kambam–Painavu–Trichur shear zone, *M–A* Moyar–Attur shear zone, *P–C* Palghat–Cauvery shear zone

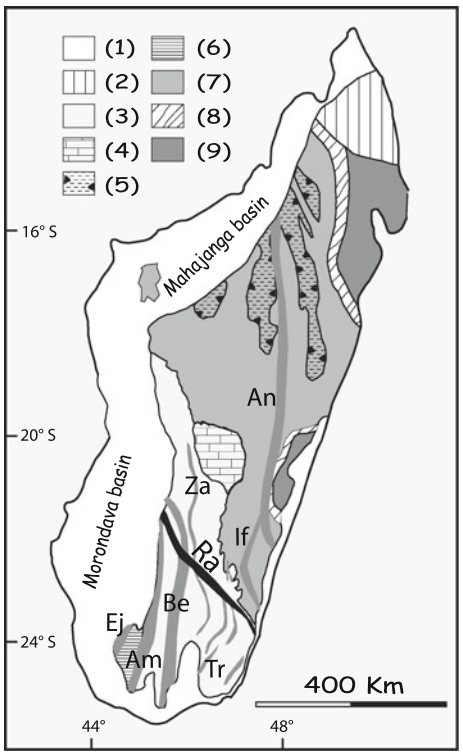

Fig. 2 Simplified geology of Madagascar (after Besairie 1969/1970 and Collins and Windley 2002). Superposed are major zones with subvertical foliation domains that have been interpreted as late Neoproterozoic/Cambrian ductile shear zones in earlier studies (compiled after Martelat 1998; Martelat et al. 2000; Nédélec et al. 2000; de Wit et al. 2001). *Am* Ampanihy shear zone, *Be* Beraketa shear zone [referred to as Vorakafotra shear zone in Rolin (1991) and de Wit et al. (2001)], *An* Angavo shear zone, *Ej* Ejeda shear zone, *If* Ifanadiana shear zone, *Ra* Ranotsara shear zone, *Tr* Tranomaro shear zone belt, *Za* Zazafotsy shear zone, Legend key: *1* Phanerozoic cover, *2* Bemarivo Belt, *3* Proterozoic supracrustal units of the SW-Madagascar Block, *4* Itremo Group, *5* Tsaratanana Sheet, *6* Vohibory Complex, *7* Antananarivo Block, *8* Betsimisiraka Suture, *9* Antongil Block

to the east and west coasts of the Malagasy microcontinent, a large number of studies have used the Ranotsara shear zone as a piercing point in Gondwana reconstructions.

The Ranotsara shear zone has been correlated with various ductile shear zones in southern India (Fig. 1), e.g., the Achankovil Shear Zone (Drury et al. 1984; Kriegsman 1993, 1995; Paquette et al. 1994; Windley et al. 1994; Shackleton 1996; Windley and Razakamanana 1996; Martelat 1998; Rajesh et al. 1998; Rajesh and Chetty 2006), the Palghat-Cauvery shear zone (de Wit et al. 1995; Janardhan 1999; Janardhan et al. 1997; Harris 1999), the Bhavani shear zone (Katz and Premoli 1979; Agrawal et al. 1992), and the Karur–Kambam–Painavu–Trichur shear zone (de Wit et al. 2001; Collins and Windley 2002; Ghosh et al. 2004).

Different correlations have also been proposed for the extension of the Ranotsara shear zone into eastern Africa (Fig. 1). Kriegsman (1993, 1995) matches the Ranotsara shear zone with the Surma shear zone, whereas Shackleton (1996) and Müller (2000) trace the Ranotsara shear zone into the parallel Aswa shear zone (also known as Aswa-Nandi shear zone). Windley et al. (1994) consider that both the Surma and the Aswa shear zones are viable candidates for an extension of the Ranotsara shear zone. Martelat (1998), in contrast, suggests that the Mt. Kenya shear zone (also known as Athi-Ikutha shear zone) represents the lateral continuation of the Ranotsara shear zone.

Various authors interpret the Ranotsara shear zone not only as a megascale ductile shear zone, but also as a structure that divides the Malagasy crystalline basement into two very different parts (Tucker et al. 1999), regions (Rambeloson 1999), blocks (Katz and Premoli 1979) or terranes (Müller et al. 1997; Chetty et al. 2003). According to Tucker et al. (1999), the Ranotsara shear zone divides the Malagasy shield into a southern part underlain predominantly by Proterozoic rocks from a northern part consisting predominantly of Late Archean crust, with a variable but undetermined extent of Middle Archean crust. Rambeloson (1999) considers that the oldest rocks south of the Ranotsara shear zone are of Palaeoproterozoic and Mesoproterozoic age, whereas to the north of the Ranotsara shear zone the rocks are as old as Archean with the exception of the Proterozoic Itremo Group. According to Katz and Premoli (1979) the ductile shear zone separates a southern charnockitic block from a gneiss terrain to the north. Chetty et al. (2003) suggests that the Ranotsara shear zone is a terrane boundary separating a region with Neoproterozoic crust to the south from Archean crust to the north.

In this paper, we assess the nature and significance of the Ranotsara shear zone and adjacent areas in more detail using remote sensing data and field-based investigations, including structural, morphological, and apatite fission track studies. As we will show in the following, our results put the Ranotsara shear zone in a different perspective. Therefore, we prefer the more neutral term "Ranotsara Zone" and will only use the term Ranotsara shear zone if it is used as such in previous studies.

Regional setting

The Precambrian to early Cambrian high-grade metamorphic rocks of southern Madagascar (here referred to as "basement") are bordered to the east by a narrow strip of Cretaceous volcanics along the coast and to the west by late Paleozoic to Recent sedimentary and volcanic rocks of the Morondava Basin (Fig. 3). In the far south of the island, the 4,000-km^2 Volcan de l'Androy complex represents a >2-km-thick sequence of interbedded basalt and rhyolite that erupted in Cretaceous times (Storey et al. 1995; Mahoney et al. 2008). The thick white line in Fig. 3 marks the location of the NW–SE trending Ranotsara shear zone as proposed in earlier studies. It extends from the southeast coast toward the Morondava basin, passing close to the villages of Ranotsara and Ihosy with the Ranotsara plain just N of the Ranotsara Zone.

The finite strain pattern in the basement rocks of southern Madagascar is thought to reflect a polyphase deformation history (Rolin 1991; Martelat et al. 2000; de Wit et al. 2001). Martelat et al. (2000) recognize two main phases of ductile deformation (D1 and D2): subhorizontal first-phase tectonic foliations with E–W stretching lineations are overprinted by D2 that is partitioned between a network of anastomosing vertical shear zones (including the Ranotsara shear zone with a proposed sinistral shear sense) and intervening fold domains. In this scenario, all major N–S striking shear zones in southern Madagascar and the NW–SE striking sinistral Ranotsara shear zone formed coevally during the second phase (D2) of transpressional deformation (Martelat et al. 2000). Th–U–Pb monazite ages were used to bracket D1 at c. 590–530 Ma and D2 at c. 530–500 Ma (Martelat et al. 2000). De Wit et al. (2001), however, interpret the finite-strain pattern in southern Madagascar as the result of two phases of early simple shear deformation between 647 and 627 Ma, followed by shortening during a third phase (corresponding to D2 of Martelat et al. 2000) between 609 and 607 Ma that resulted in the formation of the prominent N–S high-strain zones (e.g. Ampanihy and Beraketa zones). De Wit et al. (2001) consider that ductile deformation along the sinistral Ranotsara shear zone occurred during a fourth phase at c. 550–520 Ma.

North of the Ranotsara Zone, two major geological domains can be distinguished: the Antananarivo Block (Kröner et al. 2000) to the east consisting predominantly of rocks of magmatic origin and the SW Madagascar Block

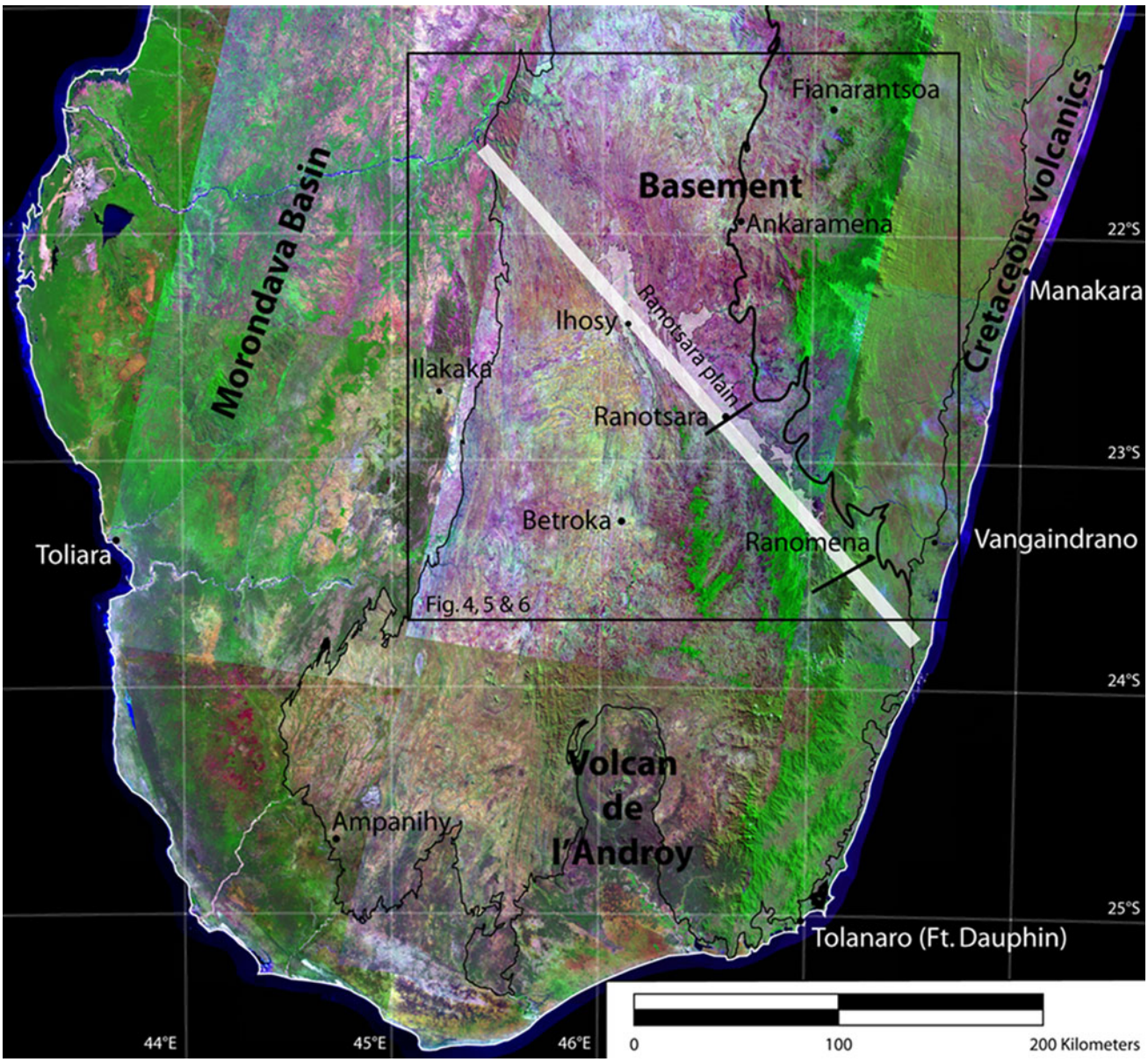

Fig. 3 Landsat ETM+ false-color composite image of southern Madagascar (bands 7, 4, and 1 = *red*, green, and blue). *Thick light-colored line* represents the orientation of the Ranotsara shear zone in previous studies, with the Ranotsara plain (*light-shaded overlay*) mostly to the NE of this line. *Thin black line* is the contact between Precambrian/Cambrian basement rocks and Phanerozoic volcanic and sedimentary rocks. *Two straight black lines* represent transects near Ranotsara and Ranomena where samples for apatite fission-track analysis were taken. *Thick black line* within the basement is a major tectonic contact between Antananarivo Block to the east and units of the southwest Madagascar Block to the west (after Giese 2009). Note the change in overall orientation of this contact from north to south

comprising mainly Proterozoic metasedimentary rocks. The boundary between the two domains is marked by a tectonic contact, which can be traced over hundreds of km. The contact has an overall N–S orientation in central southern Madagascar, but turns into a more NW–SE orientation east of Ihosy as it extends toward the southeast coast. The contact between the two blocks remains north of the Ranotsara Zone (Fig. 2).

Petrological studies indicate that most of the basement rocks north and south of the Ranotsara Zone have undergone regional granulite facies metamorphism (e.g., Ackermand et al. 1989; Nicollet 1990). Early studies yielded temperature estimates at around 750 ± 50°C and decreasing peak pressures from 1 GPa in the west to 0.4 GPa in the east (Nicollet 1990; Martelat et al. 1997). Later studies by Markl et al. (2000), however, suggest that the basement rocks in southern Madagascar share a very similar P–T evolution, with an early HT/HP event at 880 ± 60°C at 0.8 ± 0.1 GPa and a later MT/MP event at 690 ± 40°C and 0.4 ± 0.1 GPa. Petrological studies and

electron probe monazite dating of basement rocks near the Ranotsara Zone by Berger et al. (2006) reveal different monazite age populations. A population at c. 560–550 Ma is associated with granulite facies metamorphism (850–950°C and 1 GPa) that is probably related to crustal thickening. A younger population at c. 500–490 Ma is associated with a second metamorphic event at 650–730°C and 0.5 GPa, which is interpreted to be related to the D2 of Martelat et al. (2000).

Exhumation of the basement rocks commenced in the Paleozoic and is evident at the margin of the southern part of the Morondava basin, where Carboniferous deposits (part of the Sakoa Group) rest unconformably on Precambrian basement rocks (Wescott and Diggens 1997). Thermal modeling on the basis of apatite fission-track analysis suggests that parts of the basement in southern Madagascar close to the Morondava basin had already cooled to temperatures below c. 110°C in Devonian times (Seward et al. 2004). Intracontinental rifting in the Morondava basin commenced in the early Permian and resulted in local pull-apart basins (Bremer 2005). This rift system failed in the Late Triassic (Geiger et al. 2004). Based on sedimentological and seismic evidence from the Morondava Basin, Geiger et al. (2004) suggest that a short-lived episode of rifting in the Late Liassic (c. 175 Ma) was followed by continental separation and drifting of Madagascar from eastern Africa. In the Cretaceous, Madagascar separated from India. Widespread Cretaceous flood basalts along the eastern and western margins of Madagascar have been dated between c. 92 and 84 Ma (Storey et al. 1995; Torsvik et al. 1998). Storey et al. (1995) propose that the thick lava pile at Volcan de l'Androy in southern Madagascar marks the center of the Marion hot spot at c. 88 Ma. They consider that this mantle plume was responsible for continental breakup, which separated India from Madagascar.

Since middle Miocene times, Madagascar has been undergoing east–west extension (Rakotondrampiana et al. 1999) and small sedimentary basins have formed that are bordered by north–south trending faults and filled with Neogene to Quaternary sediments, e.g., the Ankay-Alaotra basin in north-central Madagascar (Laville et al. 1998) and the basins in the central highlands (Ankaratra region) near Antsirabe (Lenoble 1949; Mottet 1978). The flat-lying Ranotsara plain straddles the Ranotsara Zone to the northeast, extending from NW of Ihosy to ca. 30 km NW of Ranomena (Fig. 5). The Ranotsara plain is underlain by poorly consolidated sediments and is considered to be an internal basin of Neogene age (Hottin 1976). The sediments consist of laterized sandstones and sandy shales with intercalated layers of calcareous shales (Razafimanantsoa et al. 1972). Madagascar is presently seismically active with most seismicity confined to the crust (Rambolamanana et al. 1997; Bertil and Regnoult 1998). Seismicity is most frequent beneath the Ankaratra volcanic field in central Madagascar (Bertil and Regnoult 1998). The ongoing extension in Madagascar has been tentatively linked to the East African rift system (Bertil and Regnoult 1998; Laville et al. 1998; Kusky et al. 2007).

During its long and complex geological history, the presently exposed Precambrian basement of southern Madagascar has undergone both ductile and brittle deformations. Ductile deformation at high-grade metamorphic conditions dominated in latest Neoproterozoic to early Paleozoic times (Martelat et al. 2000; Berger et al. 2006). Brittle deformation in the basement rocks of southern Madagascar may have started already in Devonian times and continues until today. In an attempt to better characterize the deformation in the Ranotsara zone and to separate the ductile deformation history of the region from the brittle deformation history, we applied remote sensing and field-based studies.

Remote sensing data

Remote sensing is a powerful tool for geological investigations and has been applied in numerous studies for lithological mapping and for mapping morphologically defined structures. We used both optical (Landsat 7 ETM+, ASTER) and microwave (JERS-1 SAR, SRTM) space-borne remote sensing data.

Landsat 7 ETM+ is an optical imaging system with four bands (bands 1–4) in the visible and near infrared (VNIR) region of the electromagnetic spectrum with a spatial resolution of 30 m, two bands (bands 5–6) in the short wave infrared (SWIR) region with 30 m spatial resolution, one band (band 7) in the thermal infrared (TIR) region with 60 m spatial resolution, and one panchromatic band (band 8) with 15 m spatial resolution. Each Landsat 7 ETM+ scene covers an area of 180 × 180 km. The Landsat ETM+ images used in this study are all cloud-free level 1B data and cover southern Madagascar completely. A Landsat 7 ETM+ false-color composite image mosaic was created from individual scenes using bands 7, 4, and 1 for the Red, Green, and Blue layers. The raster cell resolution is 30 m.

The Advanced Spaceborne Thermal Emission and Reflectance Radiometer (ASTER) is a high-resolution optical imaging system with 14 spectral bands in three separate subsystems: three bands (bands 1–3) in the VNIR with a spatial resolution of 15 m, six bands (bands 4–9) in the SWIR with 30 m spatial resolution and five bands (bands 10–14) in the TIR region with 90 m spatial resolution. Each ASTER scene covers an area of 60 × 60 km. The ASTER data used in this study are level 1B data and

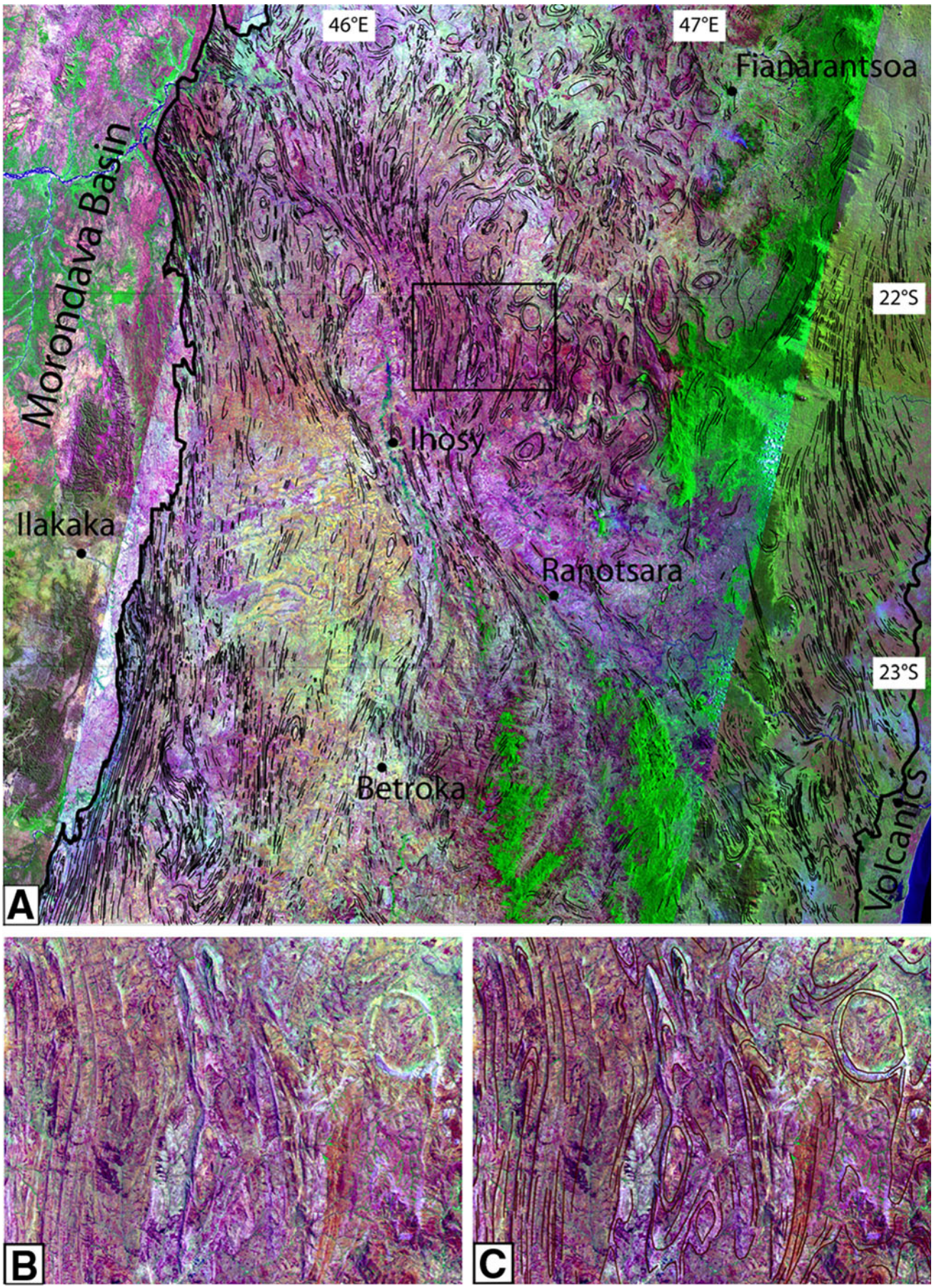
46°E
47°E
Fianarantsoa
Morondava Basin
22°S
Ihosy
Ilakaka
Ranotsara
23°S
Betroka
Volcanics
A
B
C

◀ **Fig. 4** **a** Interpreted foliation traces overlain on Landsat ETM+ false-color composite image (741 = RGB) of the Ranotsara Zone and adjacent areas. Foliation traces shown are based on interpretations of ASTER data at 15 m spatial resolution, Landsat ETM+ data at 30 m resolution, JERS-1 SAR data at 18 m resolution, and on field studies. *Rectangle* shows location of figures at bottom, (**b**) and (**c**) Detail of **a** with un-interpreted (**b**) and interpreted (**c**) image showing large-scale, dominantly N–S trending isoclinal folds and dome-and-basin-like structures

cover most of the Ranotsara zone. The ASTER data provide improved spatial and radiometric resolution and more spectral information content in comparison with Landsat ETM+ data.

The Japanese Earth Resources Satellite (JERS-1) carried an L-band (23 cm) synthetic aperture radar (SAR) system operating with HH polarization. The radar system had a ground resolution of 18 m and covered a swath width of 75 km at a look angle of 35°. Individual JERS-1 SAR scenes were assembled into a mosaic that covered entire southern Madagascar.

The Shuttle Radar Topography Mission (SRTM) is a single-pass interferometric SAR system, which collected data aboard a Space Shuttle mission in February 2000. The technology permitted the computation of digital elevation models for about 80% of the Earth's surface. The SRTM data version 4 used in this study are digital elevation data with a spatial resolution of 90 m and were provided in 5° × 5° tiles (Reuter et al. 2007; Jarvis et al. 2008). These tiles were assembled into a mosaic covering southern Madagascar.

All remote sensing data are referenced to UTM Zone 38 South with WGS-84 datum. Remote sensing data were processed with Erdas Imagine® 9.2 software and used in conjunction with geographic information system software (ArcGis® 9.2) and GeoRover™ software. GeoRover™ is a software tool that enhances the geological mapping and interpretation process. It permits, for example, a multiple windows graphical user interface that allows visualisation of up to four different, georeferenced raster data sources.

Remote sensing analysis and field-based studies

The remote sensing data mentioned above were used to map structural features in the Ranotsara zone and surrounding areas. Landsat ETM+ data were used to produce Red–Green–Blue (RGB) 7-4-1 false-color composite images for lithological discrimination and structural features. ASTER 8-4-2 and 3-2-1 (RGB) false-color composite images proved to be useful for structural and lithological mapping, whereas JERS-1 SAR images proved to be useful for structural mapping. The SRTM DEMs were useful for portraying drainage networks and for delineating structures.

In a first step, we extracted lineaments and interpreted them as foliations (tectonic and non-tectonic foliations) or fractures. In a second step, the separation in the two types of lineaments was verified in selected areas in the field and the nature of the foliations and fractures was determined wherever possible. Our main focus in the remote sensing analyses was on structural mapping (Figs. 4, 5) and less on producing lithological maps. By tracing foliations, it is possible to construct fold axial traces (Fig. 6).

Foliation traces dominantly trend roughly N–S (Figs. 4, 6). However, there are regions in the investigated area where the foliations show important changes along strike or define different geometric patterns. In the region E of longitude 47° along the east coast the trend of the foliation in the basement changes from NNE–SSW trending in the north (i.e. at latitude of ~21°S, east of Fianarantsoa) to NNW–SSE to NW–SE trending from 22°30′S on southwards (see also Raharimahefa and Kusky 2007).

Another region where the foliation traces change their along-strike orientation is across the central segment of the Ranotsara zone (from about 50 km NW of Ihosy to the village of Ranotsara (Figs. 4, 6). Here, the overall N–S trend of the foliation traces is sinistrally deflected by about 30–40 km across the Ranotsara Zone. Within the central segment of the Ranotsara Zone the foliation traces strike NW–SE to NNW–SSE, whereas they curve back into a N–S orientation outside the zone.

Circular and elliptical shapes can be outlined in the region W and SW of Fianarantsoa extending as far south as the Ranotsara Zone. Figure 4b and c show a transitional domain between circular and elliptical shapes in the eastern part and more N–S striking foliation planes in the western part. Lithologically defined structures are clearly visible and can be traced over tens of kilometers. Large-scale folds with N–S trending axial planes can be distinguished. The circular and elliptical structures correspond to folded structures (see also next section), but also to intrusive bodies. Most of these intrusive bodies, however, also show evidence for large-scale folding about N–S fold axes.

Large kilometer-scale open-to-isoclinal folds are common throughout central and southern Madagascar. The fold axial traces essentially show the same pattern as the foliation traces and can clearly be followed across the northwestern and central segment of the Ranotsara Zone (Fig. 8).

Interpreted fractures are shown in Fig. 5a overlain on a Landsat 7 ETM+ mosaic. A detail of Fig. 5a is shown in the ASTER false-color composite images (R, G, B, = band 8, 4, and 2) of Fig. 5b and c. Differently oriented fracture sets can be identified, which are often geographically restricted. WNW-ESE fracture sets occur mostly in a N–S strip in the easternmost part of the basement, parallel to the east coast. E–W and NNW–SSE fracture sets dominate the

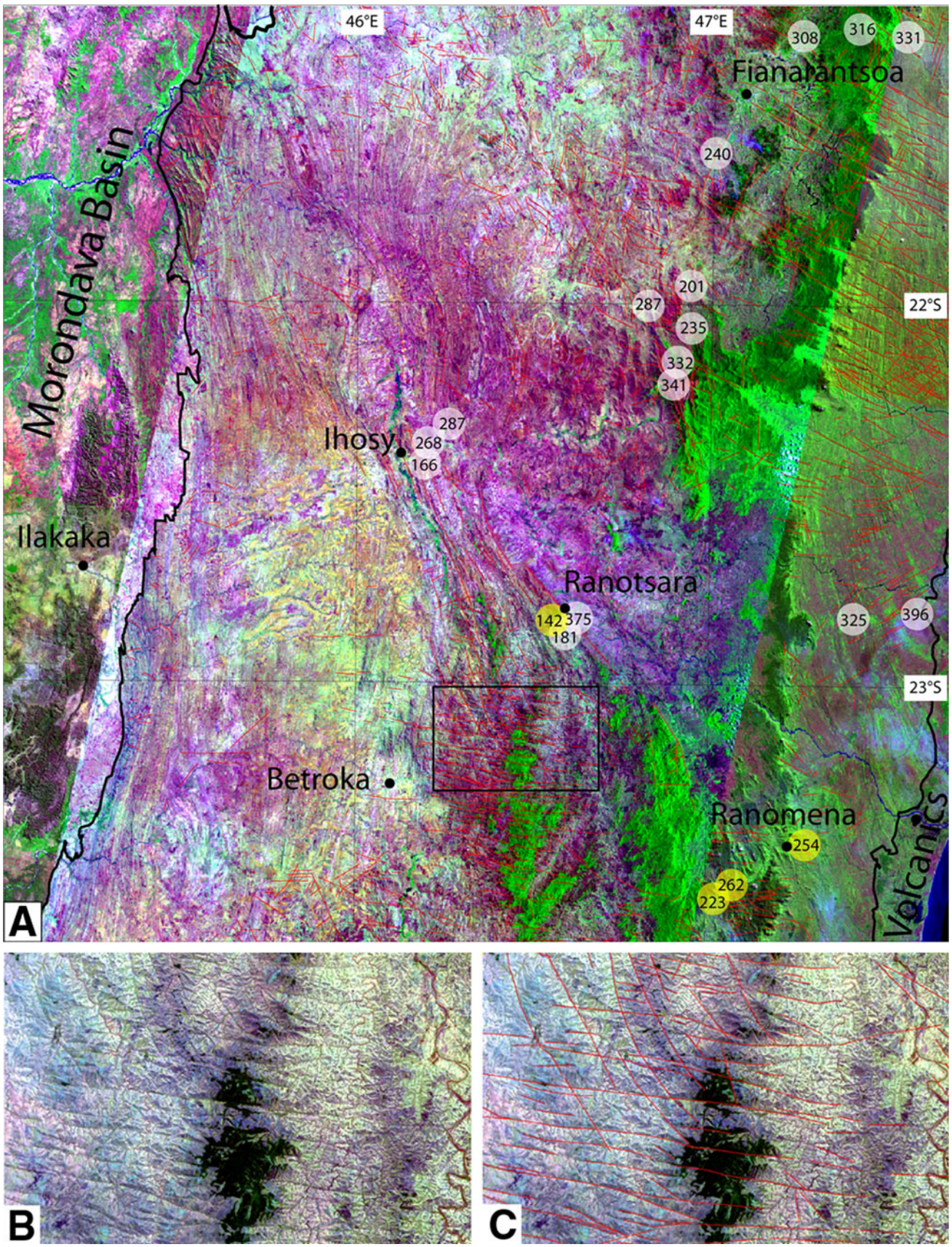
46°E
47°E
308
316
331
Fianarantsoa
240
Morondava Basin
201
287
22°S
235
332
341
287
Ihosy
268
166
Ilakaka
Ranotsara
142
375
181
325
396
23°S
Betroka
Ranomena
254
262
223
Volcanics
A
B
C

◄ **Fig. 5** **a** Fracture pattern overlain on Landsat ETM+ false-color composite image (741 = RGB) of the Ranotsara Zone and adjacent areas. Fractures shown are based on interpretations of mosaicked ASTER data at 15 m spatial resolution, Landsat ETM+ data at 30 m resolution, JERS-1 SAR data at 18 m resolution, and on field studies. Apparent apatite fission-track ages from Seward et al. (2004) and this study are shown, underlain by *white* and *yellow* dots, respectively. *Rectangle* shows location of figures at bottom; (**b**) and (**c**), Uninterpreted and interpreted ASTER false-color composite images (842 = RGB), respectively, showing two main fault sets: one striking E–W and another one striking NNW–SSE

region E of Betroka (Fig. 5b, c), whereas a NW–SE to NNW-SSE trending fracture set occurs (sub) parallel to the Ranotsara Zone. In the basement W and N of Fianarantsoa fracture sets are more variably oriented. The NW–SE to NNW–SSE fractures along the Ranotsara zone strike mostly parallel to ductile foliation planes (Fig. 6).

Field studies have been done in large parts of the inset shown in Fig. 3, with detailed studies focusing on the central segment of the Ranotsara Zone (i.e. in the area

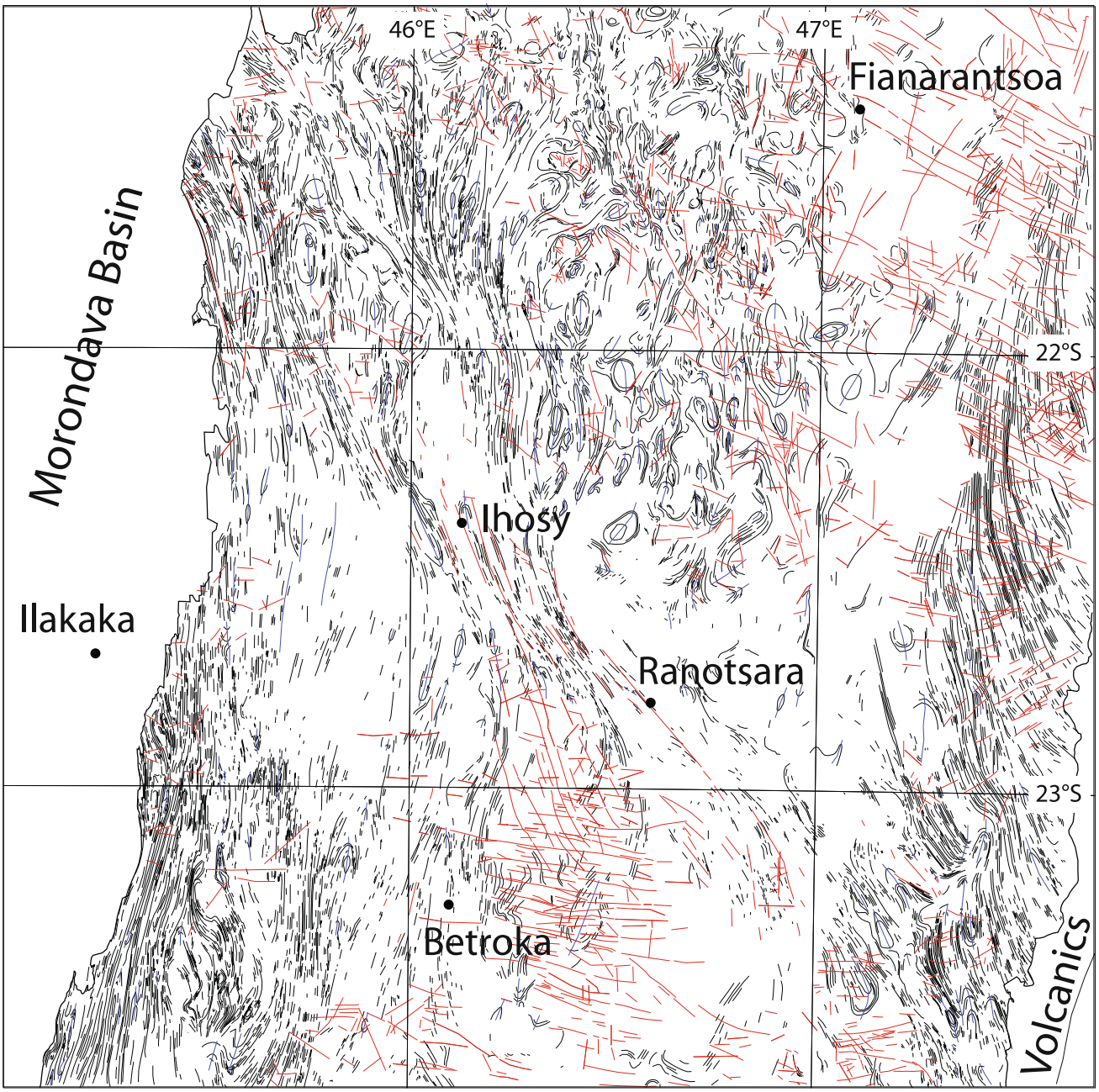

Fig. 6 Main structures of the Ranotsara Zone and surrounding areas. *Dark lines* are foliation traces, *red lines* are *brittle* fractures, and *blue lines* are axial traces of large-scale (>km-scale) folds

between the towns of Ihosy and Ranotsara) and adjacent regions on either side. Samples for apatite fission-track analysis were taken along two transects across the central and southeastern segment of the Ranotsara Zone (Fig. 3).

The basement rocks consist predominantly of para- and orthogneisses and migmatites with minor occurrences of marbles, quartzites, and micaschists. The rocks have been intensely deformed at high-grade metamorphic conditions in latest Neoproterozoic/Cambrian times at c. 550–520 Ma (e.g., Andriamarofahatra et al. 1990; Kröner et al. 1996; Martelat et al. 2000; Giese 2009; Grégoire et al. 2009) and two major ductile deformation phases and a minor late phase of localized deformation can be distinguished. The oldest recognized deformation event (here referred to as the Andreaba phase) resulted in a high-grade tectonic foliation, which is generally parallel to lithological contacts. Isoclinal Andreaba phase folds have only been observed in a few outcrops. The parallelism of lithological layering and the Andreaba tectonic foliation suggests that transposition occurred during the Andreaba phase. In areas that have undergone little subsequent overprint, the Andreaba foliation is mostly gently W-dipping and may contain a W–E to WSW–ENE oriented lineation defined by aligned biotite and elongated quartz and feldspar. This lineation is especially well developed close to the tectonic contact between the SW Madagascar Block and the Antananarivo Block, north of the Ranotsara Zone (Giese 2009). Near Ankaramena, for example, W-dipping mylonites with WSW plunging lineations display high-temperature microstructures indicating ENE-ward directed Andreaba phase thrusting of the SW Madagascar Block on top of the Antananarivo Block (Giese 2009). The Andreaba phase is overprinted by a second major deformation event, the Ihosy phase.

The intensity of the Ihosy phase varied across central-southern Madagascar. It produced high-strain domains dominated by (sub)vertical foliation planes and intervening low-strain domains where the orientation of the dominant foliation is much more variable and generally dips less steeply (e.g. in the Antananarivo Block W and SW of Fianarantsoa). The low-strain domains generally comprise large coherent bodies of granitoid rocks, in contrast to the steep domains where metasedimentary rocks dominate and granitoid rock bodies are less frequent and generally smaller in size. In the following, low- and high-strain domains refer to Ihosy phase deformation at varying intensity.

The high-strain domains with subvertical foliation planes are more or less parallel and are oriented N–S, except along part of the Ranotsara Zone where they are deflected into a NW–SE orientation. The NW–SE striking high-strain zone will be discussed in more detail in the next section. In the N–S striking high-strain domains, isoclinal Ihosy phase folds with shallow N or S plunging fold hinges and a subvertical axial planar foliation are observed at various scales. The Ihosy foliation can then only be clearly distinguished from the Andreaba foliation in the fold hinges, whereas in the fold limbs transposition has occurred and the Andreaba foliation has become parallel to the Ihosy foliation. In zones of transposition, the Andreaba lineation can no longer be discerned. Shallow N or S plunging lineations marked by the alignment of minerals such as phlogopite and sillimanite or elongated minerals such as quartz and feldspar occur in the N–S striking high-strain zones. At several localities we observe shallow N or S plunging lineations that formed by the intersection of the Andreaba and Ihosy phase foliation and are parallel to the hinges of nearby Ihosy phase folds at all scales, including km-scale upright, isoclinal folds.

In the low-strain domains with more open, upright Ihosy phase folding, the dominant foliation is represented by the Andreaba foliation. Generally, no or only a weak axial planar Ihosy phase foliation is formed in the low-strain domains and consequently intersection lineations formed by the two tectonic foliations are lacking or are only weakly developed. The older Andreaba phase lineation is generally better preserved in low-strain domains. Ihosy phase fold axes mostly plunge shallowly to the N or S in the low-strain domains and the orientation of the Andreaba lineation varies depending on its location with respect to Ihosy phase fold hinges. Andreaba lineations plunge toward the WSW to SW on W-dipping Ihosy phase fold limbs and toward the NE on E-dipping Ihosy phase fold limbs.

Fig. 7 Structures along the central segment of the Ranotsara Zone in the Ihosy-Ranotsara region. *Black lines* main foliation planes, *Blue lines* axial traces of major Ihosy phase folds, *Red lines* brittle fractures. *Green dip symbols* orientation of small-scale Analaliry phase shear zones with sinistral (S) or dextral (D) sense of shear. *Arrows* orientation of Ihosy phase lineations. Numbered *red dots* indicate locations of age determinations on undeformed pegmatoid dykes, anatectic melt veins and leucosomes that crosscut the main tectonic foliation planes: (1) Ihosy quarry (22°24′688 S, 46°09′390 E); U–Pb zircon age of 527.4 ± 2.5 Ma on a crosscutting granite (Müller 2000; Sample BM-73-97) and a $^{207}Pb/^{206}Pb$ evaporation age of 537 ± 5 Ma on an undeformed anatectic granite vein (Kröner et al. 1996; Sample Mad 66-4); (2) About 30 km ESE of Ihosy (22°29′415 S, 46°17′536 E), U–Pb zircon age of 534.6 ± 1.6 Ma on a crosscutting pegmatite (Müller 2000; Sample BM-3/B-97); (3) U–Th–Pb monazite age of 532 ± 5 Ma on a leucosome within an Analaliry phase shear zone, Sample JGI 199, 22°37′491 S, 46°10′396 E, (Giese 2009). Inset shows a stereographic projection of Analaliry phase shear zones (lower hemisphere projection) and the orientation of the inferred maximum (σ_1) and minimum (σ_3) principal stresses

Structures in the central segment of the Ranotsara Zone in the Ihosy-Ranotsara area

Structures along and adjacent to the central segment of the Ranotsara Zone are shown in Fig. 7. A high-strain domain with subvertical foliation planes striking N–S can be

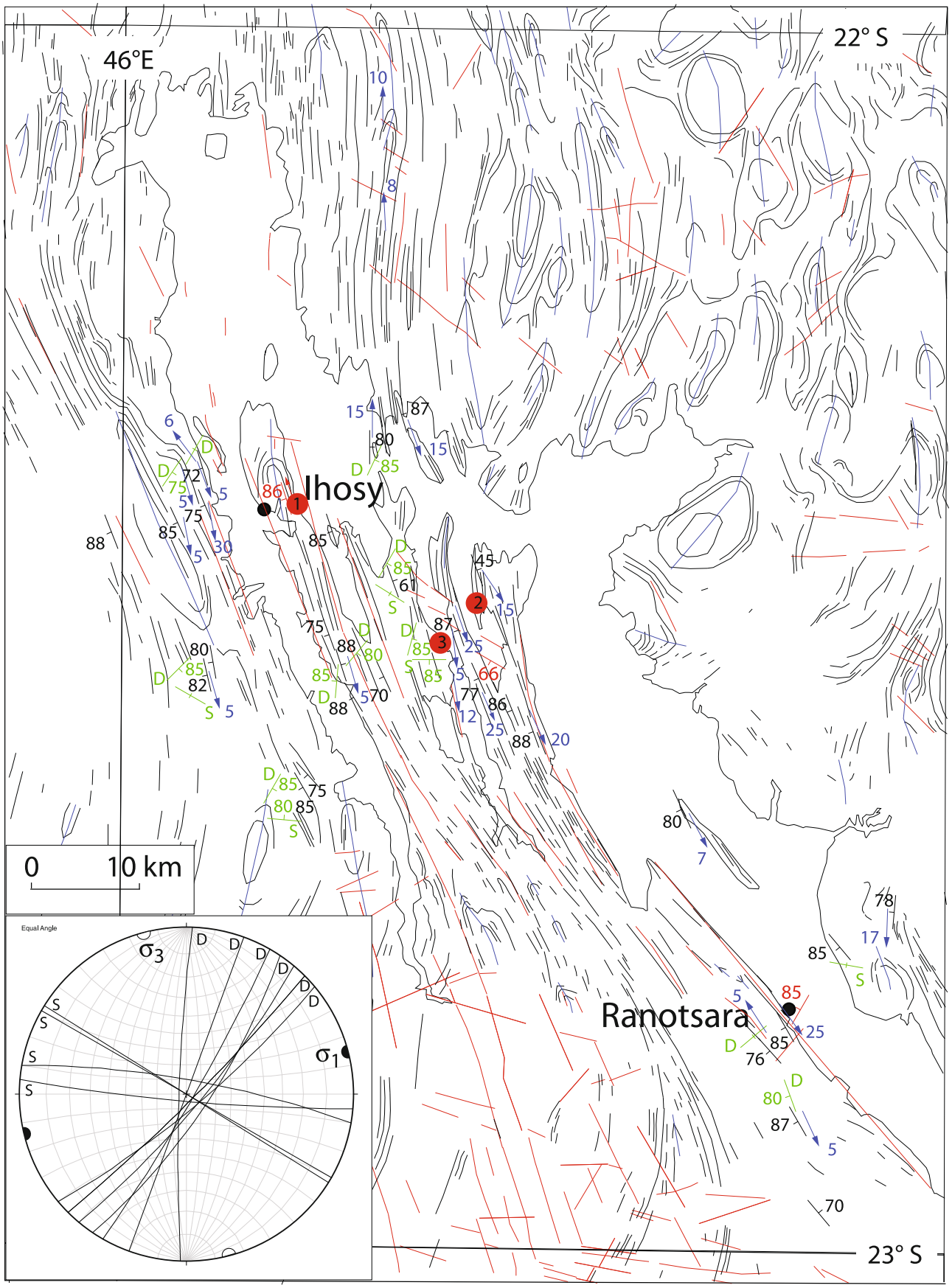
46°E
22° S
23° S
Ihosy
Ranotsara
1
2
3
0 10 km
Equal Angle
σ3
σ1
D
S

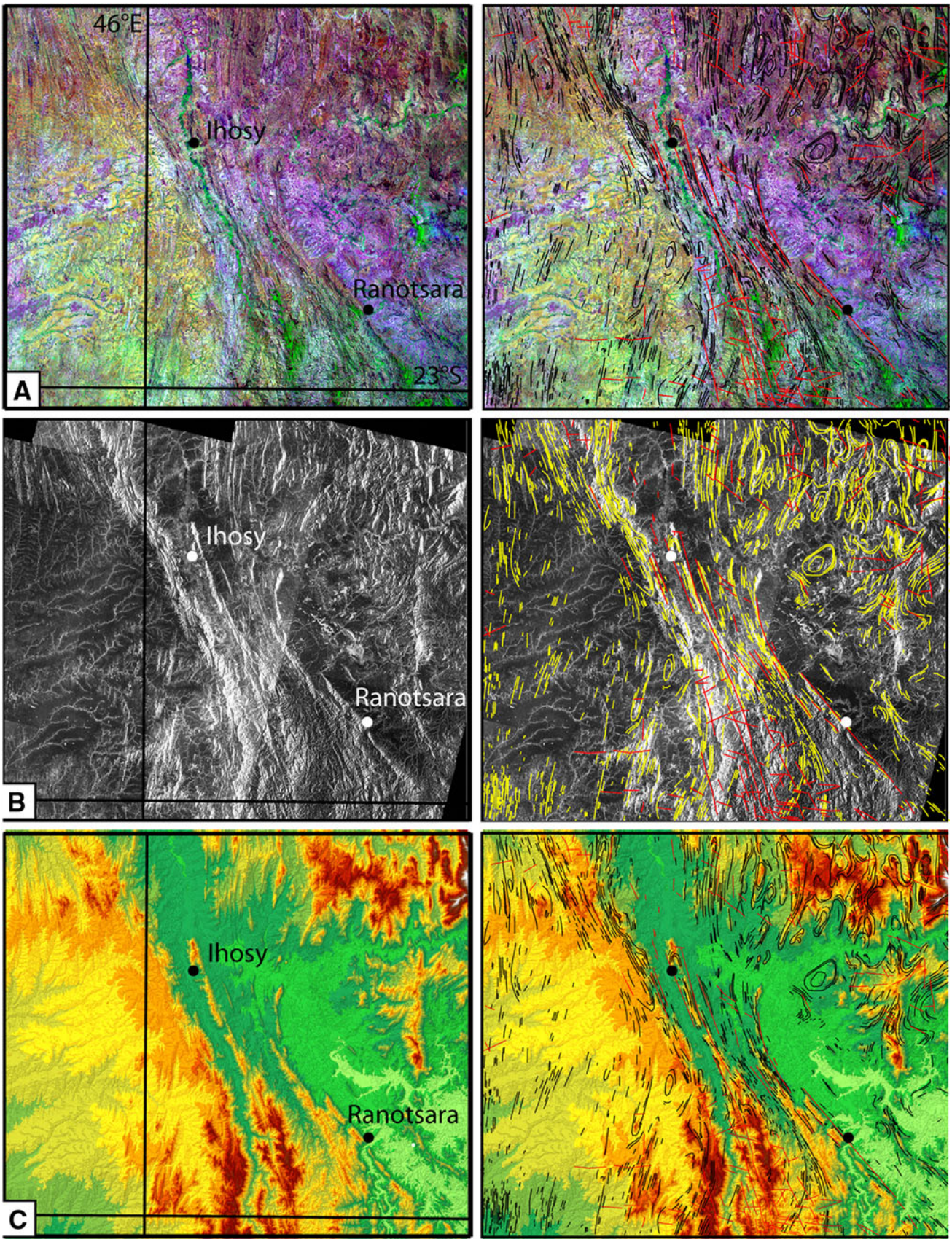
46°E
Ihosy
Ranotsara
23°S
A
Ihosy
Ranotsara
B
Ihosy
Ranotsara
C

◄ **Fig. 8** Remote sensing data of the central segment of the Ranotsara Zone. Figures on right-hand side show traces of ductile foliation planes (*black lines* in **a** and **c**, *yellow lines* in **b**) and *brittle fractures* (*red*). **a** Landsat ETM+ false-color image, RGB = 741, (**b**) JERS-1 SAR image, (**c**) SRTM digital elevation model

discerned north of the town of Ihosy (Zazafotsy shear zone of Martelat et al. 2000). Near Ihosy, this high-strain domain gradually changes its strike to NW–SE and maintains this orientation until southwest of Ranotsara where it changes its orientation to become N–S again.

The NW–SE striking high-strain domain between the towns of Ihosy and Ranotsara forms the central segment of the Ranotsara Zone and has a width of about 15 km. Planar and linear structures in this part of the Ranotsara Zone are similar to those encountered in the N–S striking high-strain domains to the north and south. Isoclinal Ihosy phase fold hinges have NW or SE shallowly plunging fold axes and subvertical NW–SE striking axial planar foliations. Except in Ihosy phase fold hinges, the Andreaba foliation is transposed and in general, nearly parallel and indistinguishable from the Ihosy foliation. Shallow NW- or SE-plunging mineral and mineral elongation lineations are present on the steep foliation planes in the NW–SE striking high-strain zone. As in the N–S striking high-strain zones, we also observe lineations that are the result of the intersection of the Andreaba and Ihosy foliation planes and are parallel to Ihosy phase fold axes at all scales. It is important to note that no mylonitic foliation overprinting Ihosy phase structures is present in the NW–SE striking high-strain zone.

The trajectories of planar structures, such as lithology, tectonic foliation, and Ihosy phase fold axial traces can be clearly followed from north to south across the central segment of the Ranotsara Zone and are only sinistrally deflected (Figs. 7, 8). Trajectories of the azimuths of Ihosy phase linear structures show the same deflection. Foliation trajectories indicate that the amount of deflection of the N–S striking foliations across the central segment of the Ranotsara Zone is about 35 km in an E–W direction.

Meter-scale shear zones containing leucosomes occur at several localities in the steep foliation domains in the Ihosy-Ranotsara region (Fig. 7). These small-scale shear zones are subvertical and clearly crosscut Ihosy phase foliations (Fig. 9), indicating that they are post-Ihosy. We refer to this minor deformation phase as the Analaliry phase. In several localities conjugate pairs of vertically oriented sinistral and dextral shear zones have been observed (Fig. 7).

The Precambrian basement rocks in and around the Ranotsara Zone are affected by brittle faulting that is often subparallel to the gneissic foliation (Fig. 6–8). Subvertical faults with subhorizontal slickenlines parallel to steep foliation planes in high-strain zones have been observed, e.g., in a quarry 2 km E of Ihosy. Steep normal faults with down-dip slickenlines occur close to the village of Ranotsara. At one locality along the Ranomena transect, a steep NW-dipping fault plane with shallow plunging slickenlines has been observed.

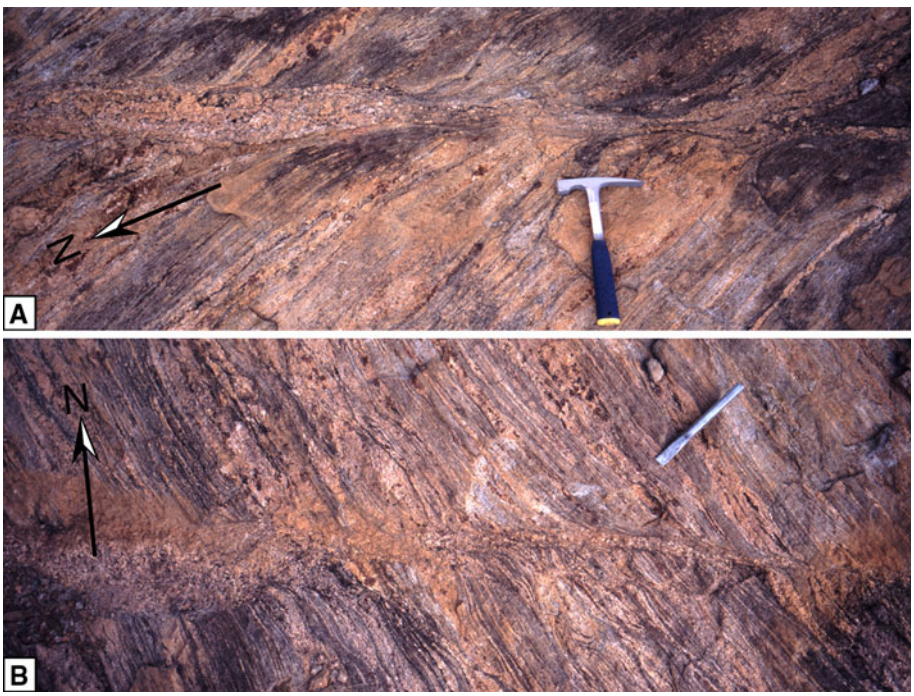

Fig. 9 Horizontal views of Analaliry phase dextral (**a**) and sinistral (**b**) shear zones with leucosomes, which intruded parallel to the shear zones. Both shear zones form part of a conjugate pair crosscutting a garnet bearing migmatitic gneiss. The main foliation dips 82° toward the WSW. Orientation of the dextral and sinistral shear zone is 135/85 (dip azimuth and dip angle) and 010/80, respectively. GPS location of outcrop: 22°31′658 S, 46°15′406 E. The crystallization age of leucosome, sampled from a similar dextral shear zone at a nearby locality (JGI_199—GPS location 22°37′491 S, 46°10′396 E), was dated by Giese (2009) at 532 ± 5 Ma (U–Th–Pb monazite age)

Table 1 Apatite fission track data from basement rocks taken along the Ranotsara and Ranomena transect

Sample No.	Latitude Longitude Altitude (m)	Rock type	Counted grains	$Rho_D \times 10^5$ cm^{-2} (counted)	$Rho_S \times 10^5$ cm^{-2} (counted)	$Rho_I \times 10^5$ cm^{-2} (counted)	U (ppm)	Mean Track length (μm), SD *c*-axis equivalent MTL (μm), SD number of confined tracks	$P(X^2)$, % Variation	Age ± 2σ, (Ma)
JGI 004	S 23.5606	Grt-Bt-Gneiss						13.72 ± 0.18 (1.72)		
	E 47.03587		20	13.00 (7820)	27.86 (2441)	25.99 (2277)	24.88	14.77 ± 0.13 (1.24)	29.41 (5.98)	222.9 ± 23
	609							96		
JGI 006	S 23.5239							12.03 ± 0.21 (2.09)		
	E 47.0868	Orthogneiss	20	13.09 (7820)	22.39 (2013)	18.00 (1618)	15.64	13.73 ± 0.13 (1.24)	9.51 (96.39)	262.4 ± 24.4
	640							102		
JGI 021	S 23.5606							11.47 ± 0.19 (2.00)		
	E 47.0359	Migmatite	20	12.94 (7820)	51.91 (2813)	42.46 (2301)	39.4	13.31 ± 0.12 (1.28)	55.18 (0)	254.0 ± 28.6
	77							107		
JG 83	S 22.8398							12.05 ± 0.25 (2.11)		
	E 46.5759	Grt-Gneiss	20	8.10 (5990)	7.91 (683)	7.49 (646)	10.26	13.68 ± 0.18 (1.68)	20.17 (38.47)	141.9 ± 18.8
	586							69		

Rho_D represents the standard track density, Rho_S and Rho_I represent spontaneous and induced track densities, respectively. *C*-axis equivalent track length conversion after Donelick et al. (1999), $P(\chi^2)$ probability according to Green (1981). Ages are presented as central ages with a 2σ error (Galbraith and Laslett 1993). Zeta = 329 ± 20 for CN5 (JG)

Apatite fission-track analysis

A previous apatite fission-track (AFT) study by Seward et al. (2004) revealed contrasting apparent ages across the central segment of the Ranotsara Zone between Ihosy and Ranotsara with apparent ages between 166 and 181 Ma directly to the south and apparent ages between 254 and 375 Ma to the north (Fig. 5). Along this segment of the NW–SE trending Ranotsara Zone ductile foliations and brittle fractures strike mostly parallel (Fig. 7). Seward et al. (2004) interpret the jump to younger ages south of the Ranotsara Zone as indicative of brittle reactivation of ductile foliation planes. We applied AFT analysis on basement samples taken along two transects across the Ranotsara Zone: the Ranotsara and Ranomena transect (see Fig. 3 for location). The main aim of the AFT study was to investigate the low-temperature thermochronological evolution of the exhuming Precambrian/Cambrian basement across the Ranotsara Zone and in particular to determine whether a jump in ages also occurs across the southeastern segment of the Ranotsara Zone. Details on sample preparation, etching, irradiation, and fission-track measurement techniques are given in Giese (2009). The results are shown in Table 1 and Fig. 10. Ages are reported as central ages (Galbraith and Laslett 1993).

Unfortunately, only one sample along the Ranotsara transect (JG 83, a garnet-gneiss) proved to be suitable for AFT dating (Fig. 7). This sample is taken just south of a prominent NW–SE striking brittle fault that separates Precambrian basement rocks from Neogene sediments of the Ranotsara plain. The apparent AFT age of 142 Ma corresponds closely to AFT ages obtained on basement samples in the same structural position (Seward et al. 2004).

Three samples along the Ranomena transect (JGI 004, JGI 006 and JGI 021) could be used for AFT dating and yield apparent AFT ages between 223 and 262 Ma (Fig. 5). The apparent ages of samples overlap within error and suggest that the apatite fission track method is either not able to resolve relative vertical movements along brittle faults in the region or that brittle faults are absent. Faults are rarely observed along the Ranomena transect, but this might be related to the poor outcrop in an area largely covered by either primary rainforest or secondary vegetation. The one steep fault that was observed, strikes at right angles to the trend of the Ranotsara Zone. Remote sensing analysis suggests that major NW–SE striking faults are absent along this part of the Ranotsara Zone and that the NW–SE striking brittle faults along the central segment of the Ranotsara Zone do not extend all the way to the southeast coast (Figs. 5, 6).

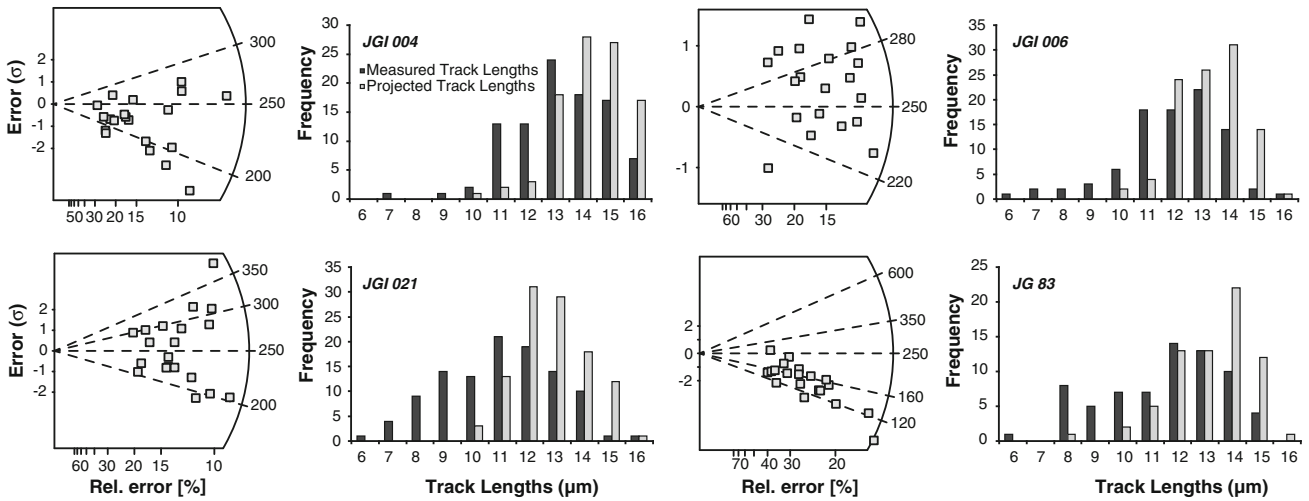

Fig. 10 Apatite fission-track data of basement samples from the Ranomena (JGI 004, JGI 006, JGI 021) and Ranotsara (JG 83) transect. Diagrams show track length distributions and a radial plot for each of the four samples

Discussion

Remote sensing and field studies in the basement rocks of central-southern Madagascar provide evidence for two major phases of ductile deformation (Andreaba and Ihosy phase), followed by a minor phase of localized deformation resulting in small-scale shear zones (Analaliry phase). The ductile deformation is subsequently overprinted by brittle deformation. The combined effects of the pronounced ductile deflection across the central segment of the Ranotsara Zone and brittle faulting along most of its length resulted in an overall NW–SE linear zone across the basement of southern Madagascar (Fig. 11).

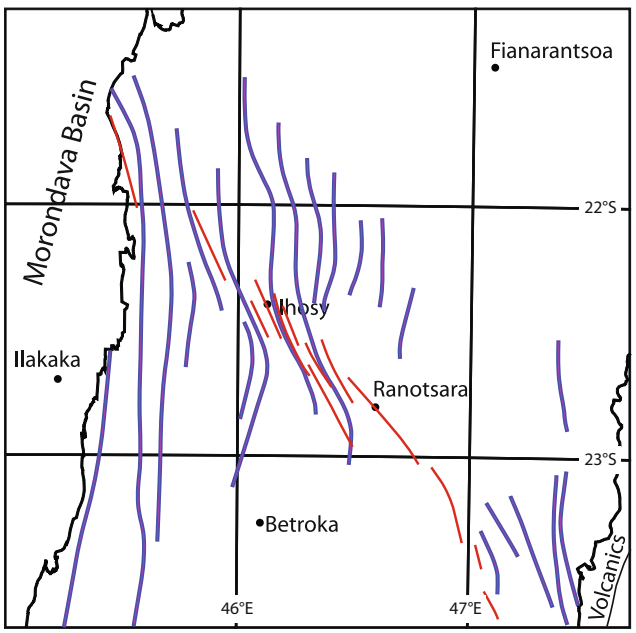

Fig. 11 Simplified structural map showing the composite nature of the Ranotsara Zone consisting of a ductile flexure along its central segment and brittle faulting along most of its length. *Blue lines* are fold axial traces of large-scale Ihosy phase folds, and *red lines* are brittle faults. The overall NW–SE orientation of the Ranotsara Zone is accentuated by foliation traces adjacent to the contact between the Antananarivo Block and the Southwest Madagascar Block near the southeast coast

Ductile deformation

The two major phases of ductile deformation in central-southern Madagascar were already recognized previously by Martelat et al. (2000) and Grégoire et al. (2009). Our Andreaba and Ihosy phase correspond to their D1 and D2, respectively. From the orientation of vertical, conjugate shear zones of the small-scale and localized Analaliry phase a regional E–W to ENE–WSW directed shortening can be deduced. The overall N–S trend of Ihosy phase folds with subvertical axial planes north and south of the Ranotsara zone indicates that the regional shortening direction during the Ihosy phase had the same orientation. The small-scale Analaliry phase shear zones seem restricted to the steep foliation domains, which contain upright, isoclinal Ihosy phase folds. We therefore propose that E–W shortening during the Ihosy phase resulted in isoclinal, upright folding and once folds locked up, additional shortening resulted in local and small-scale vertical shear zones of the Analaliry phase crosscutting the steep foliation planes. Thus, the Ihosy and Analaliry phase might be part of a progressive deformation, with the Analaliry phase recording the final ductile deformation.

Leucosomes that crystallized along small-scale shear zones of the Analaliry phase have been dated at 532 ± 5 Ma (U–Th–Pb monazite, Giese 2009) providing a lower

age limit for the Ihosy and Andreaba phase. This age is in good agreement with age data by Kröner et al. (1996), who reported a $^{207}Pb/^{206}Pb$ evaporation age of 537 ± 5 Ma for an unfoliated, fine-grained granite vein crosscutting the foliation from a quarry 2 km E of Ihosy and by Müller (2000), who gave a U–Pb zircon age of 527 ± 2.5 Ma for an undeformed granitic dyke from the same quarry and a U–Pb zircon age of 534.6 ± 1.6 Ma for an undeformed coarse-grained granitic rock, which crosscuts the foliation in the Ranotsara Zone about 20 km ESE of Ihosy (Fig. 7). U–Pb monazite and zircon analysis by Andriamarofahatra et al. (1990) on an undeformed granodiorite from the quarry E of Ihosy yielded a slightly older age of 561 ± 12 Ma.

Excluding the minor Analaliry phase, the finite ductile strain in central-southern Madagascar resulted from the superposition of two major deformation phases. The shape of the finite strain ellipsoid and thus the orientations of tectonic foliations and lineations depend on the history of the two deformation phases. During the Andreaba phase, a subhorizontal tectonic foliation with a subhorizontal lineation formed, probably as a result of shearing with a significant non-coaxial component and vertical flattening. This subhorizontal foliation was overprinted by progressive E–W directed coaxial shortening during the Ihosy phase, producing low-strain zones with upright, open folds and high-strain zones with upright, isoclinal folds and a subvertical axial planar foliation.

Ramsay and Huber (1983) show that second-phase progressive horizontal shortening of a first-phase horizontal foliation formed by flattening deformation may result in the development of complex linear fabrics. Progressive horizontal shortening during the second phase forms a new vertical tectonic foliation, which is axial planar to upright folds and is at right angles to the initial horizontal orientation of the first-phase foliation. The intersection of the two foliations produces subhorizontal intersection lineations that are parallel to the hinge lines of second phase folds. Depending on the strain intensity, the progressive horizontal shortening may even produce subhorizontal elongation lineations that may be parallel to the intersection lineations and parallel to the hinges of second-phase folds (Ramsay and Huber 1983). The fact that Ihosy phase intersection lineations, elongation lineations, and fold axes in the N–S striking high-strain domains of central-southern Madagascar are generally subparallel and shallowly plunging indicates that they formed as the result of the superposition of two major deformation phases (Andreaba and Ihosy phase), whose axial planes were initially intersecting at nearly right angles. Thus, we emphasize that the Ihosy phase subhorizontal lineations in the steep high-strain zones cannot be used to infer a tectonic transport direction.

Lithologies, Ihosy phase foliation and lineation trajectories, and fold axial traces can be clearly traced from north to south across the central segment of the Ranotsara Zone, where they are deflected by about 35 km in E–W direction. The continuation of lithological units across the central and also the northwestern segment of the Ranotsara Zone was already established by earlier workers (e.g. Besairie 1964; Bazot et al. 1971; Bazot 1975; Hottin 1976), definitely excluding an interpretation of the Ranotsara Zone as a terrane boundary.

The steep N–S striking high-strain zones with shallow N or S plunging Ihosy phase lineations are gradually deflected into the central segment of the Ranotsara Zone, where the steep foliation planes strike NW–SE and the Ihosy phase lineations plunge shallowly to the NW or SE. This gradual change in azimuth of foliations and lineations and the absence of a NW–SE striking mylonitic foliation overprinting the Ihosy phase indicate that the deflection zone along the central segment of the Ranotsara Zone cannot be interpreted as a NW–SE striking strike-slip shear zone as previously suggested (e.g. Martelat et al. 2000; Müller 2000).

The remote sensing analysis shows that Ihosy phase strain is heterogeneously distributed throughout central and southern Madagascar. Regions with open Ihosy phase folding and dome-and-basin like structures dominate in the Antananarivo Block, which contains a significant proportion of large granitoid bodies. In contrast, regions with steep foliation domains are common within the predominantly metasedimentary sequences of the SW Madagascar Block. This suggests that the development of regional strain gradients was related to differences in dominant rock type between the different blocks. The more competent, granitoid rocks of the Antananarivo Block would deform less easily than the less competent, predominantly metasedimentary sequences of the SW Madagascar Block. We therefore speculate that the deflection along the central part of the Ranotsara Zone is related to indentation of the Antananarivo Block into the SW Madagascar Block during E–W shortening associated with the East African Orogeny.

Two scenarios can be invoked to explain the geometry of the NW–SE striking deflection zone. In a first scenario, the western paleomargin of the Antananarivo Block is assumed to strike N–S prior to the Ihosy phase of deformation. Indentation of the Antananarivo Block during the Ihosy phase is associated with a progressive decrease in E–W directed shortening from N to S resulting in a passive rotation of Ihosy phase structures about a vertical axis and the formation of the deflection zone. In this scenario, the laterally varying shortening results in a vertical shear couple with E–W oriented shear zone boundaries at the N and S margins of the deflection zone. As the deflection of N–S striking foliations across the Ranotsara Zone amounts

to 35 km and the width of the deflection zone normal to the boundaries is 50 km, the shear strain related to this sinistral strike-slip shearing would be low, i.e., 0.7, and the deflection zone could be considered as the result of an incipient E–W striking shear zone. In a second scenario, the western paleomargin of the southern Antananarivo Block changes its overall strike from N–S to NW–SE at the latitude of the future deflection zone. Indentation of the Antananarivo Block during the Ihosy phase associated with laterally uniform E–W directed shortening would then result in the formation of the NW–SE striking deflection zone in the units of the SW Madagascar block. We favor the second scenario as the zone with competent granitoid intrusions in the Antananarivo block changes its overall trend from N–S to NW–SE at the latitude of the deflection zone.

Although deflection of Ihosy phase foliations suggests that the deflection zone formed syn- to late Ihosy phase, it cannot be excluded that indentation of the Antananarivo Block and initiation of the deflection zone already commenced earlier during the Andreaba phase. E–W to NE–SW oriented Andreaba phase elongation lineations can often be observed on the Andreaba foliation (e.g. Martelat et al. 2000; Giese 2009; Grégoire et al. 2009). North of the Ranotsara Zone, this lineation is especially prominent near the tectonic contact between Antananarivo Block and units of the SW Madagascar Block to the west (e.g. Itremo Group, Amborompotsy-Ikalamavony Group) and is interpreted as a tectonic transport direction (Fernandez and Schreurs 2003; Nédélec et al. 2003; Giese 2009). We propose that the three ductile deformation phases recognized in the investigated area are the result of progressive, approximately E–W oriented shortening during the East African Orogeny in latest Neoproterozoic/early Cambrian times (c. 550–530/520 Ma; Fig. 12). During the Andreaba phase, units of the SW Madagascar Block are imbricated and superposed on the Antananarivo Block (Giese 2009). Progressive shortening during the Ihosy phase resulted in upright N–S trending refolding of Andreaba phase folds, folding of tectonic contacts, and—confined to steep foliation domains—transposition of Andreaba phase folds and formation of upright, isoclinal folds with axial planar foliations. Once isoclinal folds locked up, local and small-scale (conjugate) shear zones of the Analaliry phase developed sealing the ductile deformation.

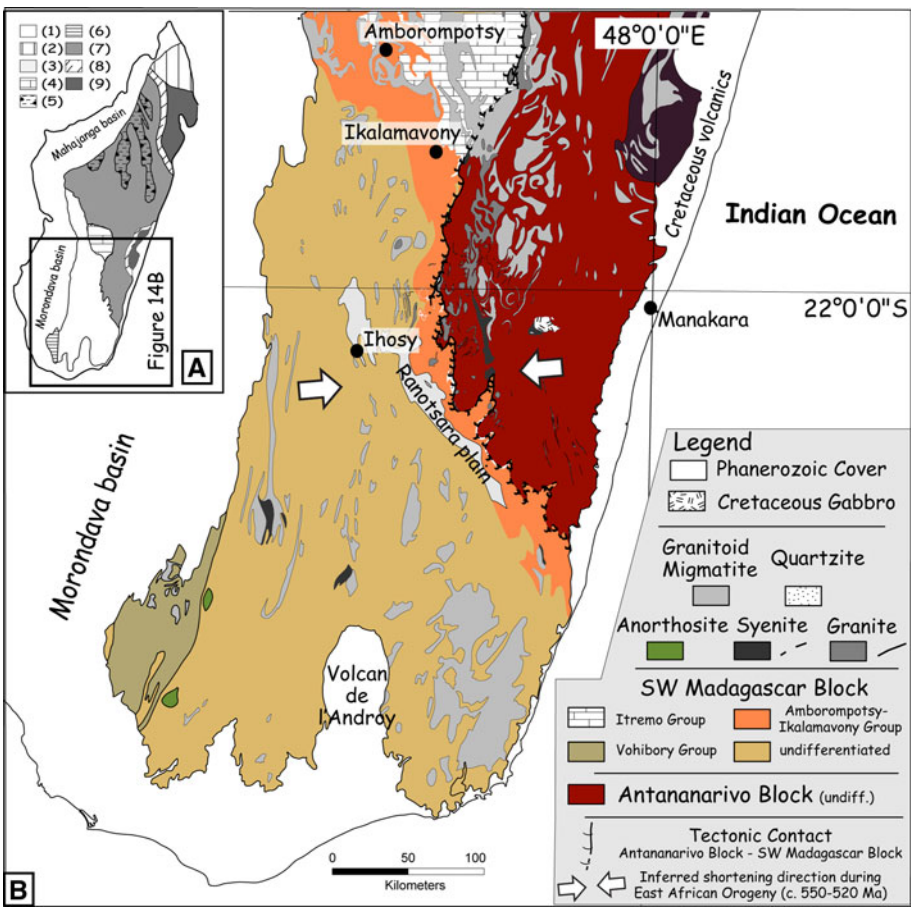

Fig. 12 **a** Geological overview map of Madagascar showing location of **b**. Legend key as in Fig. 2. **b** Simplified geological map of southern and central Madagascar showing the main units (modified after Giese 2009). The ductile, high-grade foliation pattern in the Ranotsara Zone and adjacent areas is interpreted as the result of overall E–W shortening at c. 550–530/520 Ma (Giese 2009) during the East African Orogen with indentation of the competent Antananarivo Block (and possibly adjacent units to the east, e.g. Antongil Block) into the less-competent, predominantly metasedimentary units of the SW Madagascar Block

Brittle deformation

Brittle faults and ductile foliation planes in the Ranotsara Zone often strike parallel indicating that brittle deformation preferentially reactivated zones of weakness represented by the strongly foliated ductile domains. Along the central segment of the Ranotsara Zone, brittle faults separate the Precambrian/Cambrian basement to the southwest from lower-lying, poorly consolidated alluvial and lake sediments (Besairie 1949a, b, c) of the Ranotsara plain to the northeast. NW–SE striking brittle faulting occurred along most of the Ranotsara Zone. A major NW–SE striking fault extending from 15 km NW of the village of Ranotsara to Midongy Sud had already been recognized during reconnaissance mapping of the region (Rakotondramazava et al. 1945; Besairie 1949a, b, c; Besairie et al. 1949a, b, c). Our remote sensing analysis suggests that faulting parallel to the Ranotsara Zone does not extend all the way to the southeast coast. Apatite fission track analysis across the Ranomena transect also does not provide evidence for brittle faulting along the southeastern end of the Ranotsara Zone.

The age of the onset of brittle faulting along the Ranotsara zone is poorly constrained. The sediments of the Ranotsara plain could give clues on the age of faulting, as their deposition is most likely fault-controlled. Little is known, however, about their age and thickness. Besairie (1964, 1969/1970) and Hottin (1976) inferred a Neogene and Plio-Quaternary age for these sediments, respectively. Eight shallow drill holes in the central parts of the Ranotsara plain are marked on the 1:100 000 geological maps Sahambano (Razafimanantsoa et al. 1972), Ihosy Nord (Randriamanantena et al. 1972) and Bedabo (Rakotonanahary et al. 1972). Four drill holes with a maximum depth of 48 m did not reach the basement, whereas four other drill holes with a depth between 18.3 and 50 m did penetrate the basement underlying the sediments of the Ranotsara plain (Fig. 13). These data point to a limited thickness of the sediments underlying the Ranotsara plain. This would then be in contrast with the interpretation of Emmel et al. (2004, 2006), who suggest on the basis of titanite and apatite fission-track data that an important, fault-controlled Karroo basin underlies the Ranotsara plain.

The prominent morphological expression associated with the NW–SE striking fault separating the gneisses from lower-lying alluvial sediments of the Ranotsara plain along the central segment of the Ranotsara Zone indicates that faulting is quite recent or even ongoing. Recent or active faulting is also suggested by the drainage pattern as noted earlier by Besairie (1949a) and Seward et al. (2004). The drainage pattern shows a marked bend in the course of the Sahambano, Ionaivo, and Itomampy rivers (Fig. 13). These three major rivers previously drained into the Mozambique Channel, but faulting along the Ranotsara Zone resulted in their capture by the Menarahaka and Mananara rivers flowing to the SE and draining into the Indian Ocean. Although morphology and drainage pattern point to recent

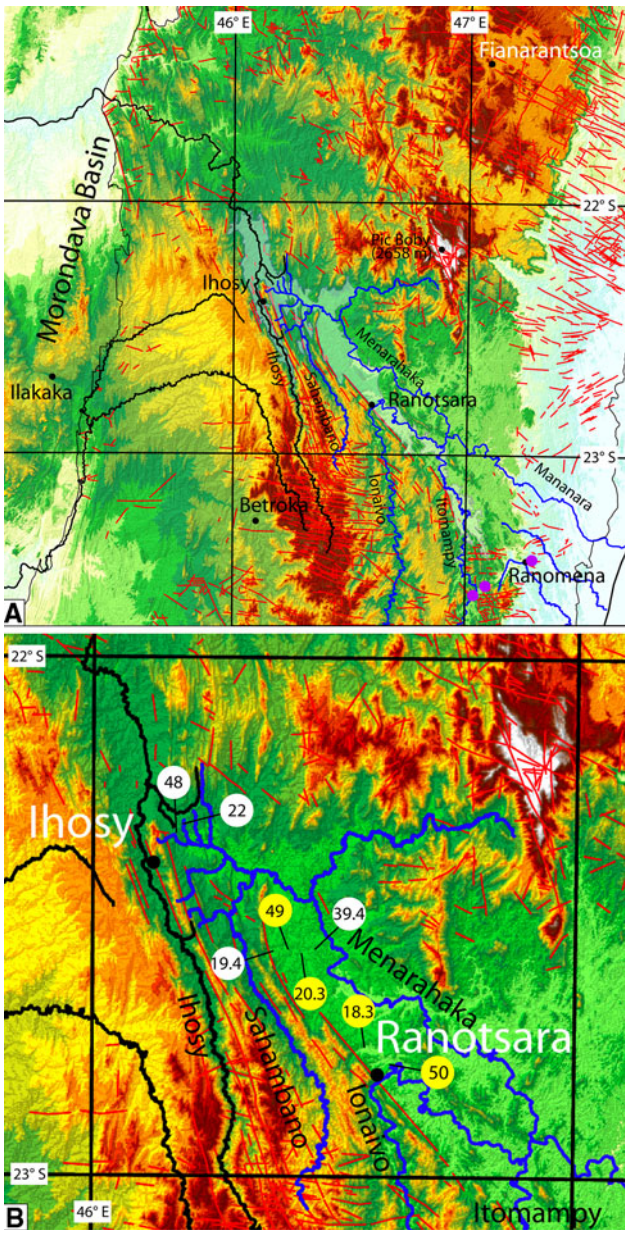

Fig. 13 SRTM based digital elevation models with drainage pattern (*black* and *blue lines*) and fracture pattern (*red lines*) overlain. Drainage pattern is based on interpretation of Landsat ETM+ and ASTER data. **a** Overview of Ranotsara Zone and adjacent areas. Outline of Neogene sediments in the Ranotsara plain (transparent overlay) after 1:100 000 geological maps of the 1960s and 1970s. Rivers draining into the Mozambique Channel are drawn in *black*, and rivers draining into the Indian Ocean are drawn in *blue*. AFT sample locations along Ranomena transect are indicated in *purple*. **b** Detail of the fault and drainage pattern in the Ihosy-Ranotsara area. *Yellow dots* indicate drill holes that penetrated into the crystalline basement, whereas *white dots* indicate drill holes that did not encounter the basement. Final depth of drill hole is given in meters

or active faulting, brittle activity probably occurred already earlier during breakup of Gondwana in the Phanerozoic as suggested by apatite fission-track data (Seward et al. 2004; Emmel et al. 2004).

Conclusions

Our remote sensing and field-based studies of southern Madagascar indicate that what formerly has been referred to as the Ranotsara shear zone is neither a major terrane boundary nor a megascale, intra-crustal strike-slip shear zone. It can therefore not be used as a piercing point in Gondwana reconstructions. Our results show that it is a composite structure, referred to by us as the Ranotsara Zone, consisting of a high-grade ductile deflection zone restricted to its central segment and NW–SE oriented low-grade brittle faulting along most of its length. The ductile component of the Ranotsara Zone developed during the East African Orogeny in latest Neoproterozoic/Cambrian times, whereas the brittle component formed during exhumation and extension in Phanerozoic times. The ductile deflection zone across the central segment of the Ranotsara Zone is interpreted as the result of indentation of the more competent Antananarivo Block into the less competent, predominantly Proterozoic metasedimentary rocks of the SW Madagascar Block during E–W to ENE–WSW (present-day coordinates) shortening related to the East African Orogeny.

Acknowledgments Financial support by the Swiss National Fund (grants 2000-65306/01, 200020-105453/1, 200020-118023/1) is gratefully acknowledged. Apatite fission-track analysis by JG was carried out at the fission-track laboratory of the ETH Zürich headed by Diane Seward. The authors thank Colin Reeves for providing the Gondwana reconstruction shown in Fig. 1, Michel Rakotondrazafy for kind assistance during field campaigns in Madagascar, Djordje Grujic and Marco Herwegh for providing useful comments on an earlier version of this paper, and Alan Collins and Anne Nédélec for constructive reviews.

References

Ackermand D, Windley BF, Razafiniparany A (1989) The Precambrian mobile belt of southern Madagascar. In: Daly JS, Cliff RA, Yardleys BWD (eds) Evolution of metamorphic belts. Geol Soc Spec Publ 43, pp 293–296

Agrawal PK, Pandey OP, Negi JG (1992) Madagascar: a continental fragment of the paleo-super Dharwar craton of India. Geology 20:543–546

Andriamarofahatra J, de la Boisse H, Nicollet C (1990) Datation U-Pb sur monazites et zircons du dernier episode tectono-métamorphique granulitique majeur dans le Sud-Est de Madagascar. C R Acad Sci Paris 310:(Série II) 1643–1648

Bazot G (1975) Les formations métamorphiques précambriennes du sud-est de Madagascar. Bur Rech Géol Min Deuxième Série Sect. II 6:573–590

Bazot G, Bousteyak L, Hottin G, Razafiniparany A (1971) Carte du métamorphisme de Madagascar. C R Sem Géol Madagascar 47–57

Berger A, Gnos E, Schreurs G, Fernandez A, Rakotondrazafy M (2006) Late Neoproterozoic, Ordovician and Carboniferous events recorded in monazites from southern-central Madagascar. Precambrian Res 144:278–296

Bertil D, Regnoult JM (1998) Seismotectonics of Madagascar. Tectonophysics 294:57–74

Rakotondramazava, Rajaonarivelo, Andriamampandry, Ranarison, Besairie, H (1945) Carte géologique du Sud-Sud-Est, échelle 1:500 000. Gouverneur Général de Madagascar

Besairie H (1949a) Notice explicative sur la feuille Iakora LM 56-57 (567). Carte géologique de reconnaissance (1:200 000). Imprimerie Nationale, Paris

Besairie H (1949b) Notice explicative sur la feuille Vondrozo NO 56-57 (568). Carte géologique de reconnaissance (1:200 000). Imprimerie Nationale, Paris

Besairie H (1949c) Notice explicative sur la feuille Midongy Sud NO 58-59 (588). Carte géologique de reconnaissance (1:200 000). Imprimerie Nationale, Paris

Besairie H (1964) Carte géologique de Madagascar (1:1 000 000). Service Géologique de Madagascar

Bésairie H (1969/1970) Cartes géologiques de Madagascar, Feuilles 1-8 (1:500 000). Service Géologique de Madagascar, Antananarivo

Besairie H, Rakotondramazava, Rajaonarivelo, Andriamampandry (1949a) Esquisse géologique de reconnaissance (1:200 000), Sheet Iakora 567, LM 56-57. Service des Mines de Madagascar

Besairie H, Rakotondramazava, Rajaonarivelo, Andriamampandry (1949b) Esquisse géologique de reconnaissance (1:200 000), Sheet Vondrozo 568, NO 56-57. Service des Mines de Madagascar

Besairie H, Rakotondramazava, Rajaonarivelo, Andriamampandry (1949c) Esquisse géologique de reconnaissance (1:200 000), Sheet Midongy Sud 588, NO 58-59. Service des Mines de Madagascar

Bonavia FF, Chorowicz J (1993) Neoproterozoic structures in the Mozambique Orogenic belt of southern Ethiopia. Precambrian Res 62:307–322

Bremer FH (2005) Karoo rifting im Morondava Becken, Madagaskar: Fazielle Entwicklung, Kinematik und Dynamik eines polyphasen Riftbeckens. Dissertation Technische Universität Berlin, pp 1–187

Caen-Vachette M (1979) Le Précambrian de Madagascar. Radiochronométrie par isochrones Rb/Sr sur roches totales. Rev Géol Dyn Géogr Phys 21 5:331–338

Chetty TRK, Vijay P, Narayana BL, Giridhar GV (2003) Structure of the Nagavali Shear Zone, Eastern Ghats Mobile Belt, India: Correlation in the East Gondwana reconstruction. Gondwana Res 6:215–229

Collins AS (2006) Madagascar and the amalgamation of Central Gondwana. Gondwana Res 9:3–16

Collins AS, Pisarevsky SA (2005) Amalgamating eastern Gondwana: The evolution of the Circum-Indian Orogens. Earth Sci Rev 71:229–270

Collins AS, Windley BF (2002) The tectonic evolution of central and northern Madagascar and its place in the final assembly of Gondwana. J Geol 110:325–340

De Wit MJ, Vitali E, Ashwal LD (1995) Gondwana Reconstruction of the East Africa–Madagascar–India–Sri Lanka–Antarctica fragments revised. Centennial Geocongress, extended abstracts. Geol Soc South Africa 1:218–221

De Wit MJ, Bowring SA, Ashwal LD, Randianasolo LG, Morel VPI, Rambeloson RA (2001) Age and tectonic evolution of Neoproterozoic ductile shear zones in southwestern Madagascar, with implications for Gondwana studies. Tectonics 20:1–45

Donelick RA, Ketcham RA, Carlson WD (1999) Variability of apatite fission-track annealing kinetics, II. Crystallographic orientation effects. Am Miner 84:224–1234

Drury SA, Harris NBW, Holt RW, Reeves-Smith GW, Wightman RT (1984) Precambrian tectonics and crustal evolution in South India. J Geol 92:3–20

Emmel B, Jacobs J, Razakamanana T (2004) Titanite and apatite fission track analyses on basement rocks of central-southern Madagascar: constraints on exhumation and denudation rates along the eastern rift shoulder of the Morondava basin. J Afr Earth Sci 38:343–361

Emmel B, Jacobs J, Dassinnies M, Razakamanana T (2006) The drainage system along the Ranotsara Shear Zone: an inheritance from early Gondwana break-up tectonics? In: Schwitzer C, Brandt S et al (eds) Proc German-Malagasy Research Cooperation in Life and Earth Sciences, pp 19–28

Fernandez A, Schreurs G (2003) Tectonic evolution of the Proterozoic Itremo Group metasediments in central Madagascar. In: Yoshida M, Windley BF, Dasgupta S (eds) Proterozoic East Gondwana: supercontinent assembly and breakup, vol 206. Geol Soc Spec Publ. pp 381–399

Galbraith RF, Laslett GM (1993) Statistical models for mixed fission-track ages. Nucl Tracks Rad Meas 21:459–470

Geiger M, Clark DN, Mette W (2004) Reappraisal of the timing of the breakup of Gondwana based on sedimentological and seismic evidence from the Morondava Basin, Madagascar. J Afr Earth Sci 28:363–381

Ghosh JG, de Wit MJ, Zartman RE (2004) Age and tectonic evolution of Neoproterozoic ductile shear zones in the Southern Granulite Terrain of India, with implications for Gondwana studies. Tectonics. doi:10.1029/2002TC001444

Giese J (2009) Tectonic evolution of the East African Orogen in central southern Madagascar: implications for assembly, exhumation and dispersal of Gondwana. PhD Thesis, University of Bern

Green PF (1981) A new tool at statistics in fission track dating. Nucl Tracks 5:77–86

Grégoire V, Nédélec A, Monié P, Montel J-M, Ganne J, Ralison B (2009) Structural reworking and heat transfer related to the late-Panafrican Angavo shear zone of Madagascar. Tectonophysics. doi: 10.1016/j.tecto.2009.03.009

Harris N (1999) The significance of the Palghat-Cauvery shear zone in southern India for correlations between south-west India and eastern Madagascar. Gondwana Res 2:471–472

Hottin G (1976) Présentation et essai d'interprétation du Précambrien de Madagascar. Bull Bur Rech Géol Min, Deuxième Série, Sect. IV, 2:117–153

Janardhan A (1999) Southern granulite terrain, south of the Palghat-Cauvery shear zone: implications for India-Madagascar connection. Gondwana Res 2:463–469

Janardhan AS, Anto F, Sivasubramanian P (1997) Granulite blocks of southern India: Implications for South India–Madagascar reconstruction. Gondwana Res Group Misc Publ 5:33

Jarvis A, Reuter HI, Nelson A, Guevara E (2008) Hole-filled seamless SRTM data V4, International Centre for Tropical Agriculture (CIAT). Available via http://srtm.csi.cgiar.org

Katz MB, Premoli C (1979) India and Madagascar in Gondwanaland: a fit based on Precambrian tectonic lineaments. Nature 1791:312–315

Kriegsman LM (1993) Geodynamic evolution of the Pan-African lower crust in Sri Lanka. Structural and petrological investigations into high-grade gneiss terrains. PhD Thesis, Utrecht University 114:1–208

Kriegsman LM (1995) The Pan-African event in East Antarctica: a view from Sri Lanka and the Mozambique belt. Precambrian Res 75:263–277

Kröner A, Braun I, Jaeckel P (1996) Zircon geochronology of anatectic melts and residues from a high-grade pelitic assemblage at Ihosy, southern Madgascar: evidence from Pan-African granulite metamorphism. Geol Mag 133:311–322

Kröner A, Hegner E, Collins AS, Windley BF, Brewer TS, Razakamanana T, Pidgeon RT (2000) Age and magmatic history of the Antananarivo Block, central Madagascar, as derived from zircon geochronology and Nd isotopic systematics. Am J Sci 300:251–288

Kusky TM, Toraman E, Raharimahefa T (2007) The Great Rift Valley of Madagascar: an extension of the Africa-Somali diffusive plate boundary? Gondwana Res 11:577–579

Lardeaux JM, Vidal G, Rakotondrazafy R (1997) Lithospheric tectonic structures developed under high-grade metamorphism in the southern part of Madagascar. Geodin Acta 10:94–114

Lardeaux JM, Martelat JE, Nicollet C, Pili E, Rakotondrazafy R, Cardon H (1999) Metamorphism and tectonics in southern Madagascar: an overview. Gondwana Res 2:355–362

Laville E, Pique A, Plaziat J-C, Gioan P, Rakotomalala R, Ravololonirina Y, Tidahy E (1998) Le fosse méridien d'Ankay-Alaotra, témoin d'une extension crustale récente et actuelle à Madagascar. Bull Soc Géol France 169:775–788

Lawver LA, Gahagan LM, Dalziel IWD (1999) A tight fit-Early Mesozoic Gondwana, a plate reconstruction perspective. Mem Natl Inst Polar Res Spec Issue 53:214–229

Lenoble A (1949) Les depots lacustres pliocènes-pleistocènes de l'Ankaratra (Madagascar). Anns Géol du Service des Mines XVIII:9–82

MacDonald D, Gomez-Perez I, Franzese J, Spalletti L, Lawver L, Gahagan L, Dalziel I, Thomas C, Trewin N, Hole M, Paton D (2003) Mesozoic break-up of SW Gondwana: implications for regional hydrocarbon potential of the southern South Atlantic. Mar Petrol Geol 2:287–308

Mahoney JJ, Saunders AD, Storey M, Randriamanantenasoa A (2008) Geochemistry of the Volcan de l'Androy basalt-rhyolite complex, Madagascar Cretaceous igneous province. J Petrol 49:1069–1096

Markl G, Bäuerle J, Grujic D (2000) Metamorphic evolution of Pan-African granulite facies metapelites from southern Madagascar. Precambrian Res 102:47–68

Martelat J-E (1998) Evolution thermomécanique de la croûte inférieure du sud de Madagascar. Thèse, Université Blaise Pascal, Clermont Ferrand II, pp 1–232

Martelat J-E, Nicollet C, Lardeaux JM, Vidal G, Rakotondrazafy R (1997) Lithospheric tectonic structures developed under high-grade metamorphism in the southern part of Madagascar. Geodin Acta 10:94–114

Martelat J-E, Lardeaux J-M, Nicollet C, Rakotondrazafy R (2000) Strain pattern and late Precambrian deformation history in southern Madagascar. Precambrian Res 102:1–20

Mosley PN (1993) Geological evolution of the late Proterozoic "Mozambique Belt" of Kenya. Tectonophysics 221:223–250

Mottet G (1978) L'Ankaratra et ses bordures (Madagascar)—Recherches de géomorphologie volcanique, Thèse, Université Lyon III, pp 1–729

Müller BGJ (2000) The evolution and significance of the Bongolava-Ranotsara shear zone, Madagascar. Ph.D. Thesis, Rand Afrikaans University, Johannesburg, South Africa, pp 1–160

Müller BGJ, Ashwal LD, Tucker RD, Rambeloson RA (1997) The Ranotsara shear zone, central Madagascar. Gondwana Res Group Misc Publ 5:60–61

Nédélec A, Ralison B, Bouchez J-L, Grégoire V (2000) Structure and metamorphism of the granitic basement around Antananarivo: a key to the Pan-African history of central Madagascar and its Gondwana connections. Tectonics 19:997–1020

Nédélec A, Bouchez J-L, Gregoire V (2003) Quartz fabric evidence for early Pan-African penetrative east-directed shearing in the

Itremo Supracrustal Group of central Madagascar. Terra Nova 1:20–28
Nicollet C (1990) Crustal evolution of the granulites of Madagascar. In: Vielzeuf D, Vidal P (eds) Granulites and crustal evolution, Kluwer Academic Publishers, Dordrecht, pp 310–291
Paquette JL, Nédélec A, Moine B, Rakotondrazafy M (1994) U-Pb, single zircon Pb-evaporation, and Sm-Nd isotopic study of a granulite domain in SE Madagascar. J Geol 102:523–538
Raharimahefa T, Kusky TM (2007) Structural and remote sensing studies of the southern Betsimisaraka Suture, Madagascar. Gondwana Res 10:186–197
Rajesh KG, Chetty TRK (2006) Structure and tectonics of the Achankovil Shear Zone, southern India. Gondwana Res 10:86–98
Rajesh HM, Santosh M, Yoshida M (1998) Dextral Pan-African shear along the southwestern edge of the Achankovil Shear Belt, South India: constraints on Gondwana Reconstructions: a discussion. J Geol 106:105–110
Rakotonanahary, Rakotomanga, JM, Rakotoarivony, Rakotomavo G (1972) Carte géologique, Beadabo (M-56), échelle 1:100 000. Service Géologique de Madagasikara, Antananarivo
Rakotondraompiana SA, Albouy Y, Piqué A (1999) Lithospheric model of the Madagascar island (western Indian Ocean): a new interpretation of the gravity data. J Afr Earth Sci 28:961–973
Rambeloson RA (1999) Gold in Madagascar. Gondwana Res 2:423–431
Rambolamanana G, Suhadolc P, Panza GF (1997) Simultaneous inversion of hypocentral parameters and structure velocity of the central region of Madagascar as a premise for the mitigation of seismic hazard in Antananarivo. Pure Appl Geophys 149: 707–730
Ramsay J, Huber M (1983) The techniques of modern structural geology, strain analysis, vol 1. Academic Press Inc, London
Randriamanantena, Rakotondrasoa, Randrianarisoa, JD (1972) Carte géologique, Ihosy Nord (K-55), échelle 1:100 000. Service Géologique de Madagasikara, Antananarivo
Razafimanantsoa, Andrianaivo P, Raholimanga M (1972) Carte géologique, Sahambano (L-56), échelle 1:100 000. Service Géologique de Madagasikara, Antananarivo
Reeves CV, Sahu BK, de Wit MJ (2002) A re-examination of the paleoposition of Africa's neighbours in Gondwana. J Afr Earth Sci 34:101–108
Reeves CV, de Wit MJ, Sahu BK (2004) Tight reassembly of Gondwana exposes Phanerozoic shears in Africa as global tectonic players. Gondwana Res 7:7–19
Reuter HI, Nelson A, Jarvis A (2007) An evaluation of void filling interpolation methods for SRTM data. Int J Geogr Info Sci 21:983–1008
Rolin P (1991) Présence de décrochements précambriens dans le bouclier méridional de Madagascar: implications structurales et géodynamiques. CR Acad Sci Paris 312:625–629
Seward D, Grujic D, Schreurs G (2004) An insight into the breakup of Gondwana: Identifying events through low-temperature thermochronology from the basement rocks of Madagascar. Tectonics. doi:10.1029/2003TC001556
Shackleton RM (1986) Precambrian collision tectonics in Africa. In: Coward MP, Ries AC (eds) Collision tectonics. Geol Soc Spec Publ 19, pp 329–349
Shackleton RM (1996) The final collision zone between East and West Gondwana: where is it? J Aft Earth Sci 23:271–287
Stern RJ (1994) Arc assembly and continental collision in the Neoproterozoic East African Orogen: implications for the consolidation of Gondwanaland. Ann Rev Earth Planet Sci 22:319–351
Storey M, Mahoney JJ, Saunders AD, Duncan RA, Kelley SP, Coffin MF (1995) Timing of hot spot-related volcanism and the breakup of Madagascar and India. Science 267:852–855
Torsvik TH, Tucker RD, Ashwal LD, Eide EA, Rakotolosofo NA (1998) Late Cretaceous magmatism in Madagascar. Paleomagnetic evidence for a stationary Marion hotspot. Earth Planet Sci Lett 164:221–232
Tucker RD, Ashwal LD, Handke MJ, Hamilton MA, LeGrange M, Rambeloson RA (1999) U-Pb geochronology and isotope geochemistry of the Archean granite-greenstone belts of Madagascar. J Geol 107:135–153
Veevers JJ (2001) Atlas of billion-year earth history of Australia and neighbours in Gondwanaland. Geomoc Press, Sydney
Wescott WA, Diggens JN (1997) Depositional history and stratigraphical evolution of the Sakoa Group (Lower Karoo Supergroup) in the southern Morondava Basin, Madagascar. J Afr Earth Sci 24:585–601
Windley BF, Razakamanana T (1996) The Madagascar-India connection in a Gondwana framework. In: Santosh M, Yoshida M (eds) The Archaean and Proterozoic terranes in southern India within East Gondwana. Gondwana Res Group Memoir 3, pp 25–37
Windley BF, Razafiniparany A, Razakamanana T, Ackermand D (1994) Tectonic framework of the Precambrian of Madagascar and its and its Gondwana connections: a review and reappraisal. Geol Rundschau 83:642–659